

Machine Movement Prediction for Collision Avoidance

Vignesh Radhakrishnan

Master of Science Thesis



Machine Movement Prediction for Collision Avoidance

MASTER OF SCIENCE THESIS

For the degree of Master of Science in Systems and Control at Delft
University of Technology

Vignesh Radhakrishnan

August 15, 2014

Faculty of Mechanical, Maritime and Materials Engineering (3mE) · Delft University of
Technology

VOLVO

The work in this thesis was carried out at VOLVO Group Trucks Technology-Advanced Technology and Research under the Vehicle Dynamics and Active Safety department. Their cooperation is hereby gratefully acknowledged.



Copyright © Delft Center for Systems and Control (DCSC)
All rights reserved.



DELFT UNIVERSITY OF TECHNOLOGY
DEPARTMENT OF
DELFT CENTER FOR SYSTEMS AND CONTROL (DCSC)

The undersigned hereby certify that they have read and recommend to the Faculty of
Mechanical, Maritime and Materials Engineering (3mE) for acceptance a thesis
entitled

MACHINE MOVEMENT PREDICTION FOR COLLISION AVOIDANCE

by

VIGNESH RADHAKRISHNAN

in partial fulfillment of the requirements for the degree of
MASTER OF SCIENCE SYSTEMS AND CONTROL

Dated: August 15, 2014

Supervisor(s):

Dr.ir. Manuel Mazo Espinosa

Stefan Bergquist

Reader(s):

prof.dr.ir. Hans Hellendoorn

Dr.ir. Riender Happee

Abstract

Construction sites are among the most dangerous work environments. Worldwide, thousands of workers are injured or killed while working with or around machinery. For Volvo Construction Equipment, safety of the workers is one of the core values. The company strives for the vision of "Zero accidents with Volvo Group Products " through high quality and innovative products that reduce the frequency of accidents as well as their consequences. The purpose of this thesis is to provide a solution towards this vision by developing a collision avoidance system for construction machinery. This is achieved by implementing a model based deterministic threat assessment approach in which the movement predictions of the machine is calculated and evaluated to determine the risk of a collision. The important aspect of generalization has also been considered, in which a new combined machine model has been developed which can be utilized to represent the kinematics of three different types of construction machinery. The results obtained from the combined machine model are compared with true machine models. Kalman filters and their extensions used for state/parameter estimation are investigated. A new method is formulated for predicting the states using Extended Kalman filter which has been proved to be better performing than the usual prediction methods. For collision detection, an algorithm based on the separating axis theorem has been developed. The developed system is investigated and validated using real-world data. The final result obtained from the thesis was an accurate threat assessment system performing for both linear and nonlinear trajectories by utilizing only GPS signals as input and also producing real time collision detection measures.

Table of Contents

Acknowledgements	xi
1 Introduction	1
1-1 Background	1
1-2 Problem Statement	1
1-3 Limitations	2
1-4 Previous Work	2
1-4-1 Passive safety	2
1-4-2 Active Safety	3
1-5 Thesis Outline	6
2 Collision Avoidance System	7
2-1 Sensor System	8
2-1-1 Global Positioning Systems	8
2-2 Decision Making	9
3 Modeling of Construction Machinery	15
3-1 Front Only Steering machines	16
3-2 Waist Steered Machines	17
3-3 Front and Back Steer Machines	18
3-4 Generalized Model	19
3-4-1 Point Mass Models	19
3-4-2 Combined Machine Model	20
4 Kalman filters and State Estimation	27
4-1 Kalman filters for state and parameter estimation	27
4-1-1 Linear Kalman Filters	27
4-1-2 Extended Kalman filter	29
4-2 Model and Filter Validation	30

5	Threat Assessment System	35
5-1	Braking/Warning Model	35
5-1-1	Warning/Braking Model	35
5-2	Prediction Results	38
5-2-1	Prediction using Iterative Extended Kalman Filter (EKF)	40
5-3	Combined Machine Model vs True Machine Model	42
5-4	Fault Detection Based on Residual	43
5-5	Collision Detection Algorithm	44
5-6	Plots	48
6	Conclusions and Future Work	59
6-1	Results	59
6-2	Future Work	60
	Bibliography	61
	Glossary	65
	List of Acronyms	65
	List of Symbols	65

List of Figures

1-1	Roll Over Protection for Compactor: The roll over protection structure can be seen over the drivers seat	3
1-2	End Result from a Blind spot detection tool	4
1-3	Criteria table for proximity warning system[28].	4
1-4	Research sequence for control and path planning	5
2-1	Collision Avoidance System	7
2-2	Illustration of the idea behind Global Positioning System (GPS) positioning	8
2-3	DGPS Functioning	9
2-4	Comparison of different types of DGPS systems	10
2-5	In the figure, trajectories of vehicle A and B are plotted with predicted positions of A and B at $t = 2secs$. A good model of the vehicle will result in accurate prediction of the position of the vehicle. Based on the predictions , it can be calculated whether the trajectories will collide with each other or not.	12
2-6	Project Flow Diagram	13
3-1	Construction Machinery models considered for the project	15
3-2	Front Steered Machines	16
3-3	Front Steered Vehicle Model	16
3-4	Waist Steered Machines	17
3-5	Articulated Structure Without Slip	18
3-6	Compactor with front and rear steering parts	18
3-7	Kinematic Model of the front and rear steered machine.[32]	19
3-8	Construction Machinery models	21
3-9	Articulated machine	21
3-10	Modified Model of the articulated structure	22
3-11	Kinematic model	23

4-1	Estimated Heading angle comparison with True GPS Heading	32
4-2	Absolute error between estimated and true heading	33
4-3	Filtered x-y Position vs true GPS x-y Position	33
4-4	Absolute error between filtered and true GPS position	34
5-1	Conventional Collision Avoidance System (CAS) utilized in Trucks and Passenger cars consisting of two regions: Braking and Warning region	36
5-2	Reaction time according to [21]	37
5-3	Lognormal Distribution of Driver Braking Reaction Times (Histogram at 0.2 Second Intervals) [18]	37
5-4	Visual representation of the two regions	38
5-5	Real-Time Trajectories A and B on which the whole analysis has been conducted.	39
5-6	Iterative EKF calculates the new predictions for a horizon of 0.1 iterated till $t = t_{warn}$ and $t = t_{brake}$	40
5-7	Histogram Comparison of position error calculated at prediction horizon $t = t_{warn}$ for trajectory B with and without Iterative EKF	41
5-8	Histogram Comparison of position error calculated at prediction horizon of $t = t_{warn}$ (Front Steered Model)	42
5-9	Histogram Comparison of position error calculated at prediction horizon of $t = t_{warn}$ (Waist Steered Model)	43
5-10	Warning off signals when Position error increases more than a threshold value (1 meter)	45
5-11	Problem using Circles for representing Machines and their predictions	46
5-12	Separating Axis Theorem visual representation	46
5-13	A 2-D projection of a 3-D Convex Polygon	47
5-14	Non-Intersecting Polygons	47
5-15	Two Intersecting Polygons	48
5-16	Trajectory A: Error plot for Point Mass and Machine Model, for a predicted horizon $t = t_{brake}$	49
5-17	Trajectory A: Error plot for Point Mass and Machine Model, for a predicted horizon $t = t_{warn}$	50
5-18	Trajectory B: Error plot for Point Mass and Machine Model, for a predicted horizon $t = t_{brake}$	51
5-19	Trajectory B: Error plot for Point Mass and Machine Model, for a predicted horizon $t = t_{warn}$	52
5-20	Trajectory B: Error Plot calculated using iterative EKF method for both predicted horizons $t = t_{warn}$ and $t = t_{brake}$	53
5-21	Collision not detected: The polygons 1 (black) and 2 (green) do not intersect each other. On the right and left part, the projections do not overlap each other	54
5-22	Collision detected: One side of the polygon 1 (black) intersects two sides of the polygon 2 (red). On all four sides, the projections overlap each other.	54
5-23	Collision detected: Two sides of the polygon 1(black) intersects one side of the polygon 2 (red). On all four sides, the projections overlap each other.	54

5-24	Collision detected: One side of the polygon 1(black) intersects two sides of the polygon 2 (red). On all four sides, the projections overlap each other.	54
5-25	Collision not detected: The polygons 1(black) and 2 (green) do not intersect each other. On the top and bottom, the projections do not overlap each other	54
5-26	Plot describing a collision scenario of a waist steered machine with a stationary obstacle. Two parts of each of the polygon depicts the front and rear part of waist steered machine. In this scenario, the machine is simulated to collide with the obstacle. The position error at $t = t_{warn}$ is given at the top right of the plot which varies at every time sample.	55
5-27	Polygon in Green for t_{warn} and in blue for t_{brake} indicates that there is no collision detected among the predicted position and obstacle.	55
5-28	The polygon detects a collision and hence turns into red. At this moment, the system will warn the driver of a possible collision through Human Machine Interface (sound/light warnings)	56
5-29	This is a scenario when the driver does not respond to the warnings. The polygon at $t = t_{warn}$ is still in red color and continues issuing warning because the algorithm still detects a collision between the position at $t = t_{warn}$ and $t = t_{brake}$. This is done by performing the collision detection algorithm for every time sample existing between $t = t_{warn}$ and $t = t_{brake}$	56
5-30	The obstacle's presence in the braking region turns the polygon to red color. As soon as the polygon detects a collision, the machine is brought to full stop by applying its maximum deceleration force	57
5-31	The machine here is under normal working condition	57
5-32	The polygon at $t = t_{warn}$ is absent in this figure. This is where the warning is switched off because the position error crosses the threshold value, here the threshold being set at 1 meter.	58
5-33	Once the position error decreases below the threshold value, the warning is again switched on and the system operates in its normal condition	58

List of Tables

5-1	RMS Position Error Comparison for $t = t_{brake}$	39
5-2	RMS of Position Error Comparison for $t = t_{warn}$	39
5-3	RMS Position Error Comparison for $t = t_{brake}$	39
5-4	RMS Position Error Comparison for $t = t_{warn}$	39
5-5	RMS of position error for Trajectory B using Iterative EKF method	40
5-6	RMS comparison of position error calculated at prediction horizon of $t = t_{warn}$ for Front steered machine	42
5-7	RMS comparison of position error calculated at prediction horizon of $t = t_{warn}$ for articulated steered machine	43

Acknowledgements

First and foremost, I would like to thank my supervisor at VOLVO Group, Stefan Bergquist for his guidance and knowledge over the last 9 months. You have helped me stay on a collision free path throughout the project and I have greatly enjoyed working with you. Your support of my project has been invaluable and I feel privileged having worked under your leadership. Special thanks to my supervisor at Delft University of Technology, Dr. Manuel Mazo Jr. for his competent and insightful discussions and ideas.

Furthermore, I also want to thank Filip Holmqvist and all other personnel at Active Safety and Vehicle Dynamics group for making all of the days in Gothenburg, Sweden enjoyable. Finally, I would like to thank my family and friends for their love and support throughout my university studies.

Delft, University of Technology
August 15, 2014

Vignesh Radhakrishnan

... to Amma, Appa and Vani

Chapter 1

Introduction

1-1 Background

Over the years the advancement in the safety standards has been restricted to road vehicles alone. Based on the survey [2], construction machinery has been one of the significant factors contributing to the fatalities caused at construction sites. In 2011 alone, 710 fatal injuries were caused due to contact with objects and equipments out of which 388 cases were caused when the contact was with a construction machinery. One of the ways of mitigating such cases is to avoid collisions with objects and other equipments. Collision avoidance systems have already made its presence in road vehicles and according to the report by Insurance Institute for highway safety, [1] such systems help in preventing or mitigating crashes by 69%. These astonishing stats motivate the fact that such Collision Avoidance System (CAS) should also be developed for construction machinery.

The work on this thesis has been carried out at Volvo Group Trucks Technology under the department of Advanced Training and Research. Volvo Group is one of the leading companies on the construction equipment and heavy machinery market. The company's history begins back in 1950 when AB Volvo bought an agricultural machine manufacturer renamed to Volvo BM AB. The company expanded globally during the 1980s and 1990s by purchasing companies in America, Asia and Europe. Today Volvo CE's product range is of a big diversity featuring for an instance, wheel loaders, haulers, crawling and wheeled excavators, motor graders, demolition equipment and pipe layers.

1-2 Problem Statement

The intention of this thesis is to develop a safety system which could help the drivers to avoid collisions with obstacles in a construction site. The problem statement can be divided into three parts. First, to formulate a generic machine model which can be used to represent not one but a class of construction machinery. The class being considered for the thesis has three types of structures :

- Front Only Steered Machines
- Waist Steered articulated Machines
- Front and Rear Steered Machines

Second, to estimate and predict the dynamics of the machine with the aid of Global Positioning System (GPS) measurements alone. Using the GPS information, other dynamics of the machine has to be estimated and predicted. Third, using the predictions, the machine should be able to avoid collisions with static as well as dynamic obstacles. In order to achieve this, collision avoidance algorithms will be developed which will have two functionalities: issue threat warnings and brake actively when the warnings are ignored by the driver.

1-3 Limitations

The machine model developed will only consider the kinematic model of the machine consisting of the parameters namely position, acceleration, velocity, heading and steering angle. During the development of the machine model, the wheel slip angles will not be considered. The project focuses on developing collision avoidance system for low operating speeds and wheel slip doesn't play a major effect on the dynamics at low speeds. Although, including the slip produces better estimates and predictions, it increases the complexity of the model. Moreover varying wheel dimensions (Front and back wheel dimensions are different for a loader) and wheel types (Compactor has rollers instead of wheels) makes it even more difficult to model. High accuracy GPS alone will be used as the sensor for the safety system. This is not optimal since GPS will not always produce accurate measurements due to the presence of noise in the signals. However, in this work, the focus is not on developing an accurate sensor system and therefore only GPS will be used. Only situations where the GPS sensor produces correct data will be utilized for validation of the functionality.

1-4 Previous Work

There has not been much development in the safety systems for construction machinery over the past years. The following sections describe some of the existing safety features for construction machinery:

1-4-1 Passive safety

The widely used passive safety systems in the present construction machines include seatbelt and roll over protection systems. Seat belts help the driver to stay intact with the machine during roll overs or collisions. Roll over protection system help in protecting the driver from getting crushed by the machine itself during roll overs [30]. But during collisions or other critical scenarios, the machines pose greater threats to the surroundings. The statistics describe that most number of accidents are caused when workers or other vehicles are hit by the construction equipments [2]. Seat-belts and ROPS do not provide any safety to the surroundings of a machine.

Apart from these two, the other passive techniques for safety includes providing training and education to the workers as well as drivers to change behavior before the construction starts. The behavior of individuals on the work-site, however, may change due to various factors/distractions most of which cannot be foreseen.



Figure 1-1: Roll Over Protection for Compactor: The roll over protection structure can be seen over the drivers seat

1-4-2 Active Safety

The active safety in construction equipments is considered to be of two types.

- Re-Active
- Pro-Active

Re-Active

Re-active technology collects data in real-time, but requires a post data collection processing effort to convert the data into information. This information is utilized to assess the overall safety by noting any potential hazards in the operating site. After the analysis, necessary precautionary steps are taken in the future events. The same data is also used for pre-task planning, including work task force scheduling and other managerial purposes. Video cameras and 3-D Laser scanners are the widely used tools to collect the real-time data. One of the important benefits obtained from this method is the detection of blind spots. Blind spots contribute to a significant number of accidents involving the construction equipments. Extensive measurements with the help of 3-D lasers helps in determining the blind spots. Once the blind spots are studied, necessary measures are undertaken to overcome the problem[31]. Figure shows the end results obtained from the blind spot detection automation tool:

One of the major drawbacks of Re-active safety systems is that, it does not help during the occurrence of any unseen scenarios. There can be some situations which are not anticipated by the safety system and therefore it fails to provide any safety to the machine or the surroundings.



Figure 1-2: End Result from a Blind spot detection tool

Pro-Active

Pro-active technology works in real-time to warn and alert personnel of the dangers occurring at that moment. The system continuously calculates the distance between the machines and workers/vehicles. If two or more construction resources are in too close proximity to one another, the sensing technology will activate visual acoustic and vibration warnings/alert to warn workers based on data from devices called Equipment and Personal Protection Units. The proximity can be calculated using sensors like RADAR, GPS, radio transceiver tags, sonar, cameras or combination of these sensors. Based on some of the recent works, RF proximity warnings have proved to be the most efficient sensor systems. Some work on proximity warning systems can be found in [29][28]. A sample criteria for selecting proximity warning and alert technology is given in Figure 1-3:

Technology	Ultrasound	RF ultra-high frequency (UHF)	Very-high frequency (VHF)	(Stereo)/video	Optical eye-safe laser (1D/2D/3D)	Infrared
Criteria						
Objective	Distance	Proximity	Proximity	Proximity/distance	Location	Proximity
Range [m]	0–10	0–40	0–500	0–500	0–50	0–30
Accuracy of data	Low	Medium	Low/medium	Medium	Medium/high	Low
Signal bounce	High	Small	Medium/high	Small	Small	Medium
Data processing effort	Small	Small	Small	Small/high	Small/high	Small
Secure signal	Noise	Yes	Yes	No	No	No
Day vs. night	Very good	Very good	Very good	Poor	Very good	Fair/good
Signal update rate	High	High	High	High	High	High
Size and weight	Small	Small	Small	Small	Medium	Small
Installation/maintenance	Small/medium	Small/medium	Small/medium	Small/medium	Small/medium	Small/medium
Purchase cost	Small	Small	Small	Small	Medium	Small
Main barriers	Short range, noise	Proximity	Omni directional signal, proximity	Line-of-sight, segmentation	Line-of-sight, segmentation	Line-of-sight, noise
Main benefits	Inexpensive	Works in high metal areas	Long range	Location, range	Location	Inexpensive

Figure 1-3: Criteria table for proximity warning system[28].

However, such proximity warning systems have some serious drawbacks:

- Proximity warning systems are strongly affected by the environment conditions such as the humidity, temperature presence of other signal emitting devices. Construction sites usually have harsh environments which could affect the performance of the system significantly.
- Presence of metal objects in between the system can again have an adverse affect on the performance of the system

- The workers/machines are still prone to collisions. The technique used in pro-active only 'warns/alerts' other machines/workers of the threat but does not take control of the machine itself. There might be scenarios where the machines/workers avoid the warnings in which the threat of collision remains unchanged.

Most of the research work has been focused on automating the construction machinery. In [3] an experiment is conducted for automating the navigation system for a load, haul and dump truck. With the help of inertial sensors, odometer and bearing LASERS, the navigation system is designed to cope up with the vehicle slip for various kind of terrains. This works provides an idea of how a particular articulated machine is modeled and methods to estimate the unobserved parameters using an extended Kalman filter.

A similar work [4] at Lulea University of technology focuses on modeling, control and path planning of an articulated vehicle. Based on a novel error dynamics modeling approach, the nonlinear kinematic model of the vehicle has been transformed in a linear switching model representation, which also considers the effect of the slip angles. The switching modeling system is based on a switching model predictive control scheme which controls the rate of the articulated angle. The diagram Figure 1-4 describes the work flow conducted for the project.

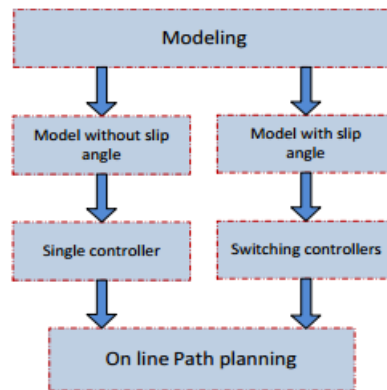


Figure 1-4: Research sequence for control and path planning

Also, with the help of this Model Predictive Control (MPC) scheme, path planning is conducted taking collision avoidance with obstacles into consideration. Similar kind of methodology is also used in [5]. Here the different kind of estimation techniques (Moving Horizon based estimation, Particle filters and Genetic algorithm based MHE) for estimating the non-direct observable states are evaluated along with the evaluation of a linear/non-linear MPC for an automated LHD machine.

The work in [6] is based on the state space approach, where the distributed position estimation problem is addressed. The transfer matrix and measurement matrix of the vehicle are established and based on vehicle dynamics and kalman filtering, the model of the state estimation and state prediction are formulated. The model for the vehicle considered here is a constant acceleration model. This work is a part of the intelligent transportation system focusing on improving the safety of road vehicles.

Work related to collision avoidance had been conducted usually under the path planning process for automated machines. For example in [7] the work is conducted to create an MPC algorithm, which is able to plan a safe and efficient path while avoiding obstacles. Both the ability to plan a path for a heavy duty vehicle and operate it along this path is investigated which also includes collision avoidance techniques. The work provides an idea about how the obstacles are represented. Various cases involving static and dynamic obstacles are taken into consideration. The work in [8] is focused on road vehicles. The work provides a description about the decision making process under different scenarios. The focus is on how to determine the threat of a collision given that the state of the obstacle is a known factor. It provides a good description about how the mitigation systems need to be integrated with the decision making process for providing an optimal control over the vehicle under different threat scenarios.

1-5 Thesis Outline

This section is intended to give a brief overview of the contents found in the chapters constituting this Master's thesis report. Chapter 2 explains the basic functionality of a collision avoidance system and the different sub systems involved in a collision avoidance system. Major emphasis is given to the threat assessment system since, the thesis is mainly based on developing the same. Also, the model based approach is explained on which the threat assessment system is developed for the thesis.

In chapter 3, kinematic modeling of the three models considered for the project are explained. In addition, a new kinematic machine model is developed which is capable to capture dynamics of the three models being considered.

Chapter 4 is devoted to the theory behind Kalman filters which are used for estimation and prediction purposes. Theory behind Extended kalman filter, an extension of kalman filter is explained followed by the algorithms involved in the filters. Followed by the explanation is the validation of the filters and the kinematic model developed in chapter 3.

Chapter 5 explains the last and final subsystem of the collision avoidance system, that is the threat assessment system. Model based approach is explained and the braking model which is utilized to calculate the predictions is described. The results are compared for two different kind of trajectories. Also, a new method for calculating the predictions is formulated and compared with the previous method for both the trajectories. The last part of the chapter consists of the algorithm used for collision detection amongst convex polygons.

The last chapter consists of the results achieved in the thesis project followed by the future work which can be performed over this project.

Collision Avoidance System

In this chapter, the basic functioning of a collision avoidance system is described. The different parts namely, the sensor systems, decision making system and the actuating system is explained. Furthermore the different parts are explained with major emphasis on the projects requirements.

Collision Avoidance System (CAS) as the name suggests are driver support systems which help in avoiding collisions by warning the driver or braking automatically with the help of real time sensor data from the environment. A basic CAS consists of the following three parts:

- Sensor System
- Decision making
- Actuators

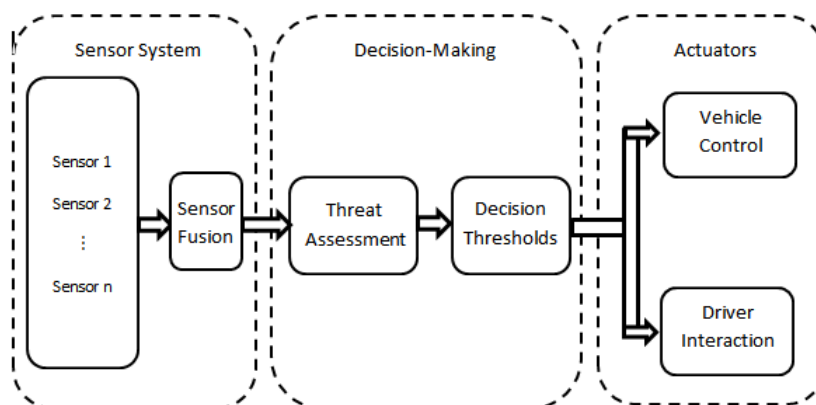


Figure 2-1: Collision Avoidance System

2-1 Sensor System

Current CAS in passenger cars and trucks utilize data from multiple sensors such as cameras, RADAR, Global Positioning System (GPS) etc. With the help of sensor data fusion, a more wider and diverse aspect of the system is measured and hence a detailed description of the environment is obtained. But it is be noted that the focus of the thesis is more toward developing an accurate decision making system and not on developing an accurate sensor technology, therefore a GPS sensor system is utilized for the project. It is assumed that the data obtained from the GPS is accurate and continuous. Developing a complex sensor system can be considered as a future scope of this project.

2-1-1 Global Positioning Systems

The Global Positioning System is a global navigation satellite system used in a vast range of both military and civilian applications where localizations and synchronization is essential. The system consists of a set of satellites which continuously transmits radio signals containing the information of the time and its orbital position. A GPS receiver is thereby able to locate itself by calculating the received signals travel time and interpret the times as imaginary spheres originating from the corresponding satellites. The intersection of those spheres define the possible positions of the receivers antenna. Figure 3-2 illustrates the principle of GPS positioning where a,b,c denotes three visible satellites and r the position of the visible antenna.

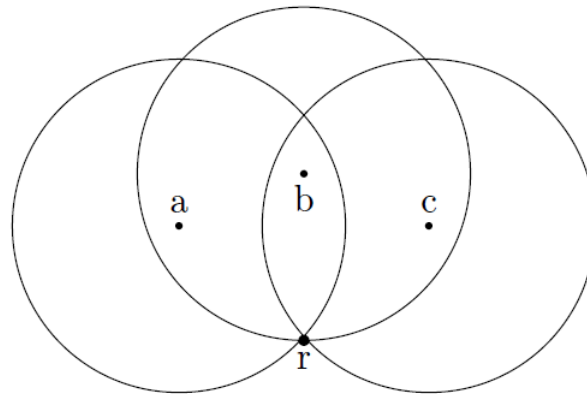


Figure 2-2: Illustration of the idea behind GPS positioning

But there are some serious drawbacks for just using the GPS technology alone for the estimation purpose. In order to compute its location in three-dimensional space, a GPS receiver must be able to lock onto signals from at least four different satellites. Moreover, the receiver must maintain its lock on each satellite's signal for a period of time that is long enough to receive the information encoded in the transmission. Achieving and maintaining a lock on four (or more) satellite signals can be impeded because each signal is transmitted at a frequency (1.575 GHz) that is too high to bend around or pass through solid objects in the signals path. For this reason, GPS receivers cannot be used indoors. Outdoors, tall buildings,

dense foliage, or terrain that stand between a GPS receiver and a GPS satellite will block the satellite's signal. Thus, in urban or heavily foliated environments a GPS receiver may be unable to provide a position fix for indefinitely long periods of time.

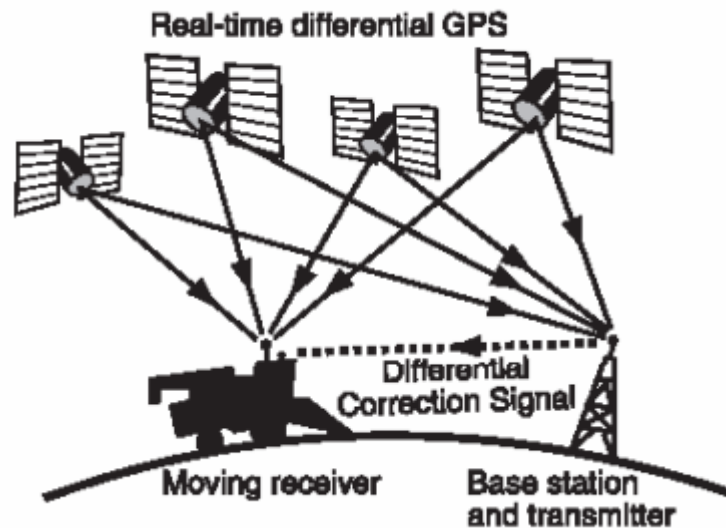


Figure 2-3: DGPS Functioning

Due to the drawbacks, a DGPS system is considered for better accuracy. Differential global positioning systems (DGPS) reduce GPS errors and provide more reliable readings. Differential correction uses a radio signal broadcast from known locations on Earth. A base station with a known location tracks the satellites and has a true range to each satellite. This information, along with its known location, is sent to the rover receiver. When the reference signal is compared to the signal received by the rover, there is a signal phase difference between the two.

2-2 Decision Making

Consisting of two parts, threat assessment and decision threshold, the decision making system interprets the estimates obtained from the sensor system to make decisions on when and how to assist the driver. The estimates are provided by the tracking system, and are used in one or more decision function to determine the appropriate collision avoidance action. One of the important tasks of this system is to determine the threat of a collision given that the state of other objects is known. Now depending on the uncertainty of state estimates obtained from the tracking system, threat assessment process can be of two types:

- Probabilistic Threat Assessment
- Deterministic Threat Assessment

	WAAS	Sub-meter	Decimeter	Centimeter- RTK
Price Range	\$100-\$500	\$500-\$2500	\$2500-\$7500	\$15,000-\$50,000
Source of Differential Signal	WAAS	Coast Guard, OmniStar VBS, StarFire I, local differential services	OmniStar HP*, StarFire II*, (requires dual-channel receiver)	Real-time kinematic systems require a base station within 6-10 miles
Accuracy	1-3 meters	1-3 feet	3-12 inches	< 1-2 inches
Advantage	Low cost, small handheld unit	Better accuracy	Best accuracy without using RTK	Highest accuracy, repeatability
Uses	Mapping, yield monitor	Mapping, yield monitor, VRT, limited guidance	Guidance (probably not row-crop), VRT	Precision guidance, elevation mapping, survey-grade mapping

Figure 2-4: Comparison of different types of DGPS systems

Probabilistic threat assessment systems as the name suggests perform decisions based on the uncertainty of the estimates obtained from the sensor system. These uncertainties are modeled using stochastic models with the help of which a probability of collision is estimated. Deterministic approach neglects the uncertainty present in the estimates. The focus is on how to determine the threat of a collision given that the state of other objects is known. One major setback using the probabilistic approach is the additional computational load. Often, stochastic models are difficult to implement in real-world applications due to the computational load and hence are restricted to theoretical findings. Hence, a deterministic approach is used in this project for decision making.

Some of the commonly used techniques for calculating the risk of a collision using both deterministic and Probabilistic methods are explained below:

TTC- Time to collision based threat assessment

Time to collision is defined as the time to contact between two objects under the assumption that the heading and velocity of both objects remain constant. Time To Collision (TTC) is a common measure for calculating the collision risk. It is also useful for illustrating and comparing the intervention timing for threat assessment algorithms in different crash scenarios.

The time for collision can be expressed as:

$$f(n) = \begin{cases} -\frac{\tilde{p}_x}{\tilde{v}_x} & \tilde{v}_x < 0 \text{ and } \tilde{a}_x = 0 \\ -\frac{\tilde{v}_x}{\tilde{a}_x} - \frac{\sqrt{\tilde{v}_x^2 - 2\tilde{p}_x\tilde{a}_x}}{\tilde{a}_x} & \tilde{v}_x < 0 \text{ and } \tilde{a}_x \neq 0 \\ -\frac{\tilde{v}_x}{\tilde{a}_x} + \frac{\sqrt{\tilde{v}_x^2 - 2\tilde{p}_x\tilde{a}_x}}{\tilde{a}_x} & \tilde{v}_x \geq 0 \text{ and } \tilde{a}_x \neq 0 \\ \text{undefined} & \tilde{v}_x \geq 0 \text{ and } \tilde{a}_x \geq 0 \\ \text{undefined} & \tilde{v}_x^2 - 2\tilde{p}_x\tilde{a}_x < 0 \end{cases} \quad (2-1)$$

Where $\tilde{p}_x, \tilde{v}_x, \tilde{a}_x$ are the relative position, velocity and acceleration, respectively. So, when the host vehicle is approaching a stationary target object with constant velocity, the time to collision is linearly decreasing with the relative position according:

$$t_{collision} = -\frac{\tilde{p}_x}{\tilde{v}_x} = \frac{\tilde{p}_x}{v_{x, host}} \quad (2-2)$$

When approaching a target the driver has can steer around the object, brake before the object or perform a combination of the two. Some work has been done based on the above technique can be found in [9][10]. The advantage with TTC based decision making algorithms is of course simplicity. However, there are several major disadvantages with such algorithms. One of the major disadvantage is that, many collisions can be avoided with moderate steering maneuvers, even at a very low TTC. Since this aspect of steering is not included in the algorithm, it is expected that the decision making algorithms solely based on TTC will generate a high number of unnecessary interventions in traffic situations that the driver considers as normal.

Required Acceleration Method

The required acceleration a_x measures the acceleration required to bring the relative velocity to zero at the time of collision.

$$a_{x, req}^{host} = sol_{a_x^{host}} \left\{ \left[\tilde{p}_x(t) \quad \tilde{v}_x(t) \right]^T = \left[0 \quad 0 \right]^T \right\} \quad (2-3)$$

where, $= sol_{a_x^{host}} \{ \dots \}$ denotes the solution with respect to the host vehicle acceleration a_x^{host} where $\tilde{p}_x(t) \geq 0$ for all t . With the assumption of constant acceleration the solution to above equation is given by solving the equation system:

$$\begin{cases} 0 = \tilde{v}_{x,0} + \tilde{a}_x t \\ 0 = \tilde{p}_{x,0} + \tilde{v}_{x,0} t + \frac{\tilde{a}_x t^2}{2} \end{cases} \quad (2-4)$$

This yields the constant acceleration required to avoid a collision, according to:

$$a_{x, req}^{host} = a_{x,0}^{obj} - \tilde{a}_x = a_{x,0}^{obj} - \frac{|\tilde{v}_{x,0}| \tilde{v}_{x,0}}{2\tilde{p}_{x,0}} \quad (2-5)$$

In the similar way, other components of acceleration can also be utilized to calculate the collision time. [8][11][12].

Potential Force

In potential field algorithms an artificial potential force acting on the host vehicle is calculated. This force is used to generate a control input to avoid any obstacle. This potential force can also be viewed as a collision decision function. A common and simple expression to calculate the potential force is given by:

$$F = -\frac{c}{\|\tilde{P}\|^i} \tilde{P} \quad (2-6)$$

where c is a constant, and $i \in N$. Potential field algorithms are common in robotic and autonomous vehicle applications. This approach was first introduced in [13], references to different applications and more sophisticated potential field algorithms than the above described method can be found in [14] [15]

Model Based Approach

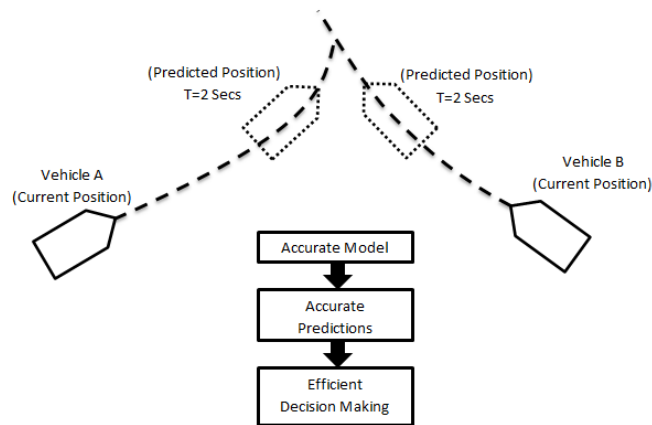


Figure 2-5: In the figure, trajectories of vehicle A and B are plotted with predicted positions of A and B at $t = 2secs$. A good model of the vehicle will result in accurate prediction of the position of the vehicle. Based on the predictions, it can be calculated whether the trajectories will collide with each other or not.

The basic idea in model based diagnosis is to compare observations of the real system with the predictions from a model. Hence, rather than calculating the TTC of the real-time machine, TTC of the future trajectories is calculated and based on this measure, different maneuvers are formulated. Automatic brake or steer interventions are then triggered to avoid or mitigate a collision when the probability of a collision is high. Both the host vehicle and the objects in the surroundings are represented as dynamic models. Figure 2-5 provides a better description of the approach. Based on the current states of the vehicle and objects, and using their dynamics model, the predictions of their future trajectories can be calculated. The accuracy of the trajectories will, to a large extent, depend upon how well the dynamics of the true system is described by the model. Generally speaking, a better model yields a better tracking performance. Hence selection of models for representing the vehicles is as important as the

decision making process. A part of the thesis is focused on developing the appropriate model of the machine for state estimation and prediction purposes.

This project is based on this approach which has proven to be of high capability [8]. The Figure 2-6 describes the basic flow involved in the project.

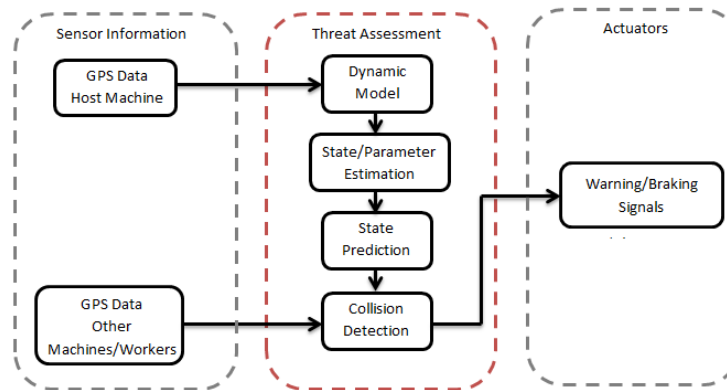


Figure 2-6: Project Flow Diagram

- **Sensor System:** As discussed in the earlier section, GPS is the only sensor system used for the project. The GPS information of the host machine along with the GPS information of the workers and other construction machines are fetched to the threat assessment system.
- **Threat Assessment System:** The threat assessment system involves a dynamic model of the machine used by a filter which estimates the missing states and parameters. Using this information the states are predicted for a varying prediction horizon. A collision detection algorithm calculates if there will be a collision between the future position of host machine and other machines/obstacles.
- **Actuator System:** Actuator systems are the final elements of the CAS which responds to the instructions provided by the threat assessment system. This is usually done by providing information of the driver through human machine interface or by taking control over the machine. This project does not consider the different aspects of the actuator system and can be seen as the future scope of this project.

Modeling of Construction Machinery

Construction machines in general is a huge class of machines ranging from large mining excavators to small loaders. This project addresses three types of construction machine model as shown in the Figure 3-1. A model describing how a machine's position and other important vehicle parameters evolve over time is an essential feature in a successful collision avoidance system. This section describes the kinematic model of the three kind of machine models. Then the aspect of generalization is addressed.


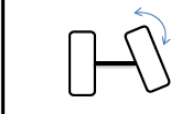

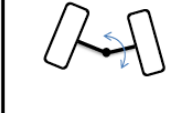

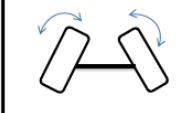
Machine Type	Simplified Model
<p>Front only steering Machine- LHD</p> 	
<p>Articulated steering Machine – Road Compactor</p> 	
<p>Front and back steering Machine- Road Compactor</p> 	

Figure 3-1: Construction Machinery models considered for the project

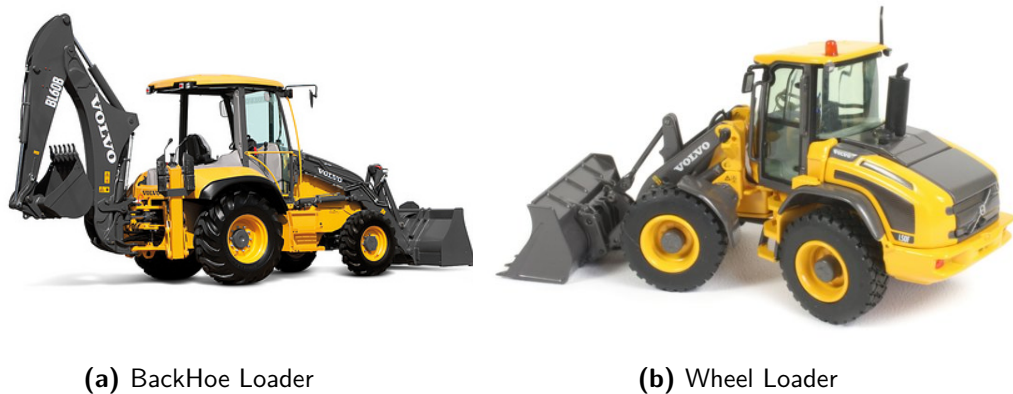


Figure 3-2: Front Steered Machines

3-1 Front Only Steering machines

This type of machines are similar to the front steered road vehicles and trucks. The driver controls the front axle of the machine to steer the vehicle. Some of the machines which are based on this type of machine models are Wheel Loaders and Backhoe Loaders. One of the common ways to represent the front steered machines is the bicycle model. Without considering the wheel slips, the kinematic model of the machine is given by:

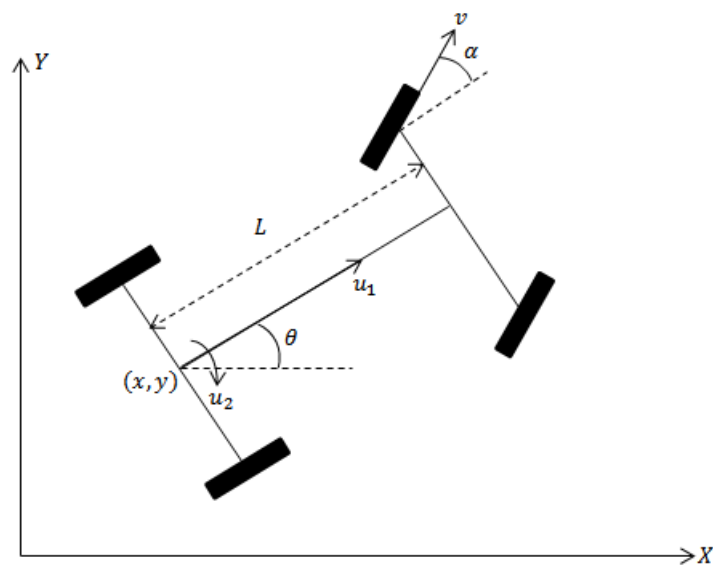


Figure 3-3: Front Steered Vehicle Model

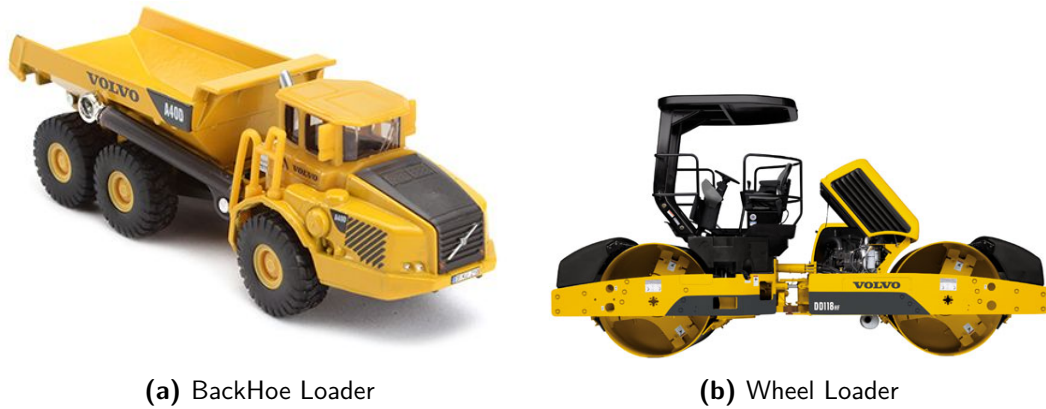


Figure 3-4: Waist Steered Machines

$$x_{k+1} = x_k + u_1 T \cos(\theta_k) \quad (3-1)$$

$$y_{k+1} = y_k + u_1 T \sin(\theta_k) \quad (3-2)$$

$$\theta_{k+1} = \theta_k + u_2 T \quad (3-3)$$

where u_1 and u_2 are the translational velocity and the angular velocity respectively. The location of the vehicle is described by the coordinates x and y and its orientation by the angle θ to the x -axis which is also considered as the heading angle of the machine. The translational and angular velocity can be formulated as:

$$u_1 = v \cos(\alpha) \quad (3-4)$$

$$u_2 = \frac{v}{L} \sin(\alpha) \quad (3-5)$$

$$(3-6)$$

where L is the distance between the steer axis and the rear axis.

3-2 Waist Steered Machines

This is a nonlinear-model designed for an articulated machine. The machine is steered with the help of the waist angle, hence the name waist steered model. It was formulated by Tokunaga and Ichihashi [27]. It consists of two moving parts: tractor and trailer. This model is more concentrated towards the relative position of the two parts with respect to a particular co-ordinate axis. Figure 3-5 describes a waist steered model without considering the body and wheel slip.

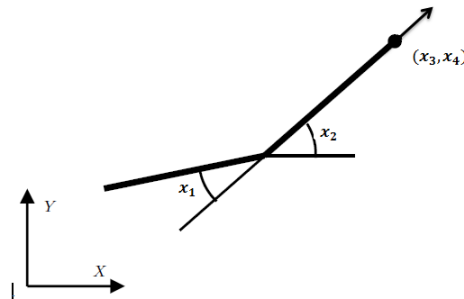


Figure 3-5: Articulated Structure Without Slip

$$x_{0_{k+1}} = x_{0_k} + \frac{v\Delta t}{l} \tan(u(t)) \quad (3-7)$$

$$x_{1_{k+1}} = x_{0_k} - x_{2_k} \quad (3-8)$$

$$x_{2_{k+1}} = x_{2_k} + \frac{v\Delta t}{L} \sin x_{1_k} \quad (3-9)$$

$$x_{3_{k+1}} = x_{3_k} + v\Delta t \cos(x_{1_k}) \sin \frac{x_{2_{k+1}} + x_{2_k}}{2} \quad (3-10)$$

$$x_{4_{k+1}} = x_{4_k} + v\Delta t \cos(x_{1_k}) \sin \frac{x_{2_{k+1}} + x_{2_k}}{2} \quad (3-11)$$

where, L is the length of the Rear part.

3-3 Front and Back Steer Machines

In such type of construction models, the machine is steered using both front and steered vehicles. The driver has control over both the steering angles. Such kind of machines are modeled using a bicycle model with two steering angles.



Figure 3-6: Compactor with front and rear steering parts

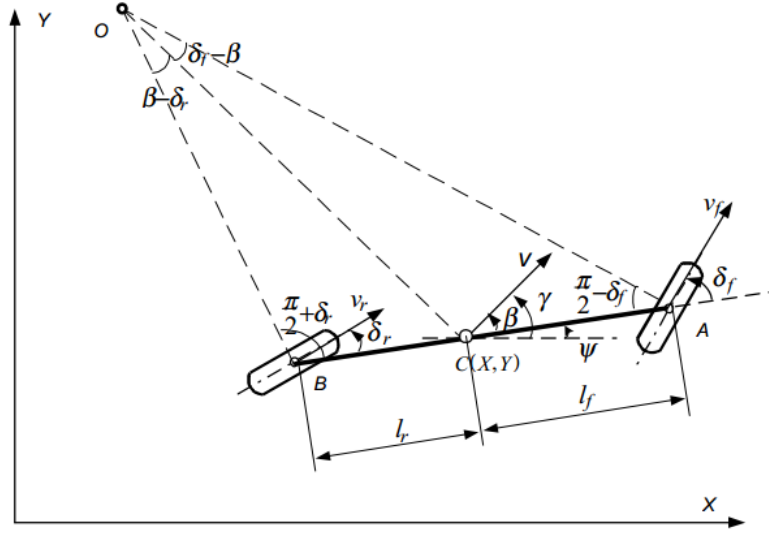


Figure 3-7: Kinematic Model of the front and rear steered machine.[32]

$$x_{k+1} = v_k \cos(\psi_k + \beta) \quad (3-12)$$

$$y_{k+1} = v_k \sin(\psi_k + \beta) \quad (3-13)$$

$$\psi_{k+1} = \frac{v_k \cos(\beta) (\tan(\delta_f) + \tan(\delta_r))}{l_r + l_f} \quad (3-14)$$

where, $\beta = \arctan \frac{l_f \tan(\delta_r) + l_r \tan(\delta_f)}{l_r + l_f}$.

In this model, there are four inputs: two steering angles, δ_f and δ_r , and two wheel velocities, v_f and v_r . The state variables of kinematic motion are the vehicle configuration (X, Y, ψ) [32].

3-4 Generalized Model

In order to develop a system which can be implemented on all three type of machines, all the three models described above has to be included in the system which will increase the complexity of the system and the computational load. Instead, a single model can be used to represent the three models described above. Two different techniques are discussed here which can be used for performing the same:

- Point mass models
- True Machine model

3-4-1 Point Mass Models

Point mass vehicle models are the simplest form of representing a moving object. The whole vehicle/body is considered to be a point mass. Hence the behavior of the point mass is studied for different type of transitions. The different scenarios are described below:

Constant Velocity Model

In this form for prediction and tracking, the vehicle is modeled as traveling at an approximately constant velocity in magnitude and direction. The transitions between different velocity are modeled by white random noise, and there is no correlation between motion in the x and y directions. The discrete model can be represented as:

$$\begin{pmatrix} P_{x_{k+1}} \\ P_{y_{k+1}} \\ V_{x_{k+1}} \\ V_{y_{k+1}} \end{pmatrix} = \begin{bmatrix} 1 & 0 & T & 0 \\ 0 & 1 & 0 & T \\ 0 & 0 & 1 & 0 \\ 0 & 0 & 0 & 1 \end{bmatrix} \begin{pmatrix} P_{x_k} \\ P_{y_k} \\ V_{x_k} \\ V_{y_k} \end{pmatrix} + \begin{pmatrix} 0 \\ 0 \\ w_x \\ w_y \end{pmatrix} \quad (3-15)$$

A model that assumes that tracked objects have constant velocity is, of course, a very simple one. In usual scenarios the vehicle undergoes varying velocity hence this model will provide inaccurate results.

Constant Acceleration/Deceleration Model

A simple extension of the above model is to add the acceleration as a state, and assume that the acceleration is piecewise constant. This model models the uncertainty of deviations from the constant acceleration by unknown driver maneuvering.

$$\begin{pmatrix} P_{x_{k+1}} \\ P_{y_{k+1}} \\ V_{x_{k+1}} \\ V_{y_{k+1}} \\ A_{x_{k+1}} \\ A_{y_{k+1}} \end{pmatrix} = \begin{bmatrix} 1 & 0 & T & 0 & \frac{1}{2}T^2 & 0 \\ 0 & 1 & 0 & T & 0 & \frac{1}{2}T^2 \\ 0 & 0 & 1 & 0 & T & 0 \\ 0 & 0 & 0 & 1 & 0 & T \\ 0 & 0 & 0 & 0 & 1 & 0 \\ 0 & 0 & 0 & 0 & 0 & 1 \end{bmatrix} \begin{pmatrix} P_{x_k} \\ P_{y_k} \\ V_{x_k} \\ V_{y_k} \\ A_{x_k} \\ A_{y_k} \end{pmatrix} + \begin{pmatrix} 0 \\ 0 \\ 0 \\ 0 \\ w_x \\ w_y \end{pmatrix} \quad (3-16)$$

For our scenario, a non-linear point mass model is considered without taking into consideration the slip involved in the wheels. The kinematic equations are given by:

$$x_{k+1} = x_k + u_1 T \cos(\theta_k) \quad (3-17)$$

$$y_{k+1} = y_k + u_1 T \sin(\theta_k) \quad (3-18)$$

$$\theta_{k+1} = \theta_k + u_2 T \quad (3-19)$$

where θ is the heading angle and u_1 is the translational velocity and u_2 is the angular velocity of the machine.

3-4-2 Combined Machine Model

This section is focused on developing a more accurate model of the machine. A single model is developed which can be utilized to represent the three models under consideration by altering some parameters. This class of construction machines involves three types of models described in the Figure 3-1.

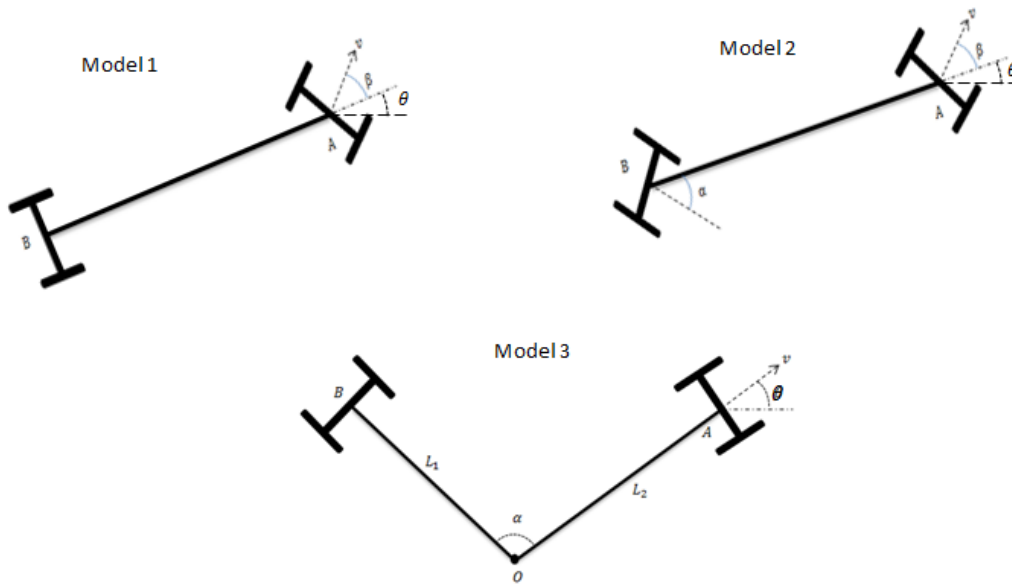


Figure 3-8: Construction Machinery models

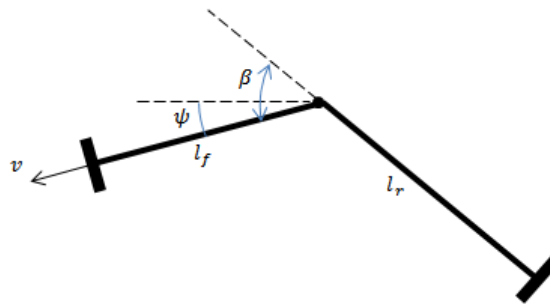


Figure 3-9: Articulated machine

The aim is to develop a model which can be used to represent all the three models. For an articulated machine as shown in model 3 of 3-8, the kinematic equations of motion when slip is not being considered are given by:

$$x_{k+1} = x_k + v_k \cdot T \cdot \cos(\psi_k) \cdot \cos(\beta) \tag{3-20}$$

$$y_{k+1} = y_k + v_k \cdot T \cdot \sin(\psi_k) \cdot \cos(\beta) \tag{3-21}$$

$$\psi_{k+1} = \psi_k + \frac{v_k \cdot T \cdot \sin(\beta)}{l_f + l_r \cdot \cos(\beta)} \tag{3-22}$$

The objective of having a generalized model can be achieved if all the three models can be derived from a common model. In order to achieve this, the points 'A' and 'B' of the structure are connected. The Figure 3-10 describes the modified model.

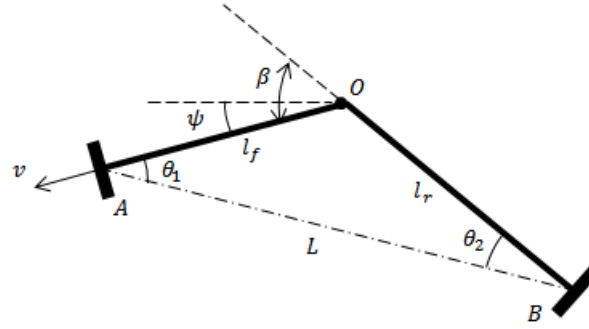


Figure 3-10: Modified Model of the articulated structure

It can be observed that in the modified model, by connecting the points A and B, the resulting structure AB with length 'L' is also the model 2 of Figure 3-8. In this model, three new variables are introduced L, θ_1, θ_2 . The interesting point to be noted here is that the three variables are a function of the articulation angle β . Now, the kinematic equations for this modified model will be derived with the three variables as a function of the articulation angle β . By deriving the kinematic model of the this modified model, it will be shown the model 1 and model 3 can also be represented as model 2 of Figure 3-8. Using the cosine rule to the triangle 'AOB' of Figure 2,

$$L = \sqrt{l_f^2 + l_r^2 - 2l_f l_r \cos(\pi - \alpha)} \quad (3-23)$$

And using the sine rule and above relationship for the same triangle,

$$\frac{l_r}{\sin(\theta_1)} = \frac{L}{\sin(\pi - \alpha)}, \quad \frac{l_f}{\sin(\theta_2)} = \frac{L}{\sin(\pi - \alpha)} \quad (3-24)$$

$$\theta_1 = \sin^{-1} \left(\frac{l_r \sin(\pi - \alpha)}{L} \right) \quad \theta_2 = \sin^{-1} \left(\frac{l_f \sin(\pi - \alpha)}{L} \right) \quad (3-25)$$

In Figure 3-11, 'N' is the instantaneous rolling center of the machine. This point is the intersection of lines 'AN' and 'BN' which are perpendicular to the orientation of the two steering parts. 'M' is the center of gravity pointed by drawing a perpendicular from the articulation point 'O' on the axis 'AB'. 'R' is the length of the line segment joining the center of gravity and the and rolling center 'N'. The velocity at the COG is perpendicular to the line segment 'OM'. The direction of the velocity at the COG with respect to the longitudinal axis of the machine is called the slip angle denoted by β .

Now applying sine rule to the triangle 'AMN',

$$\frac{L_f}{\sin(\theta_1 - \beta)} = \frac{R}{\sin(\frac{\pi}{2} - \theta_1)} \quad (3-26)$$

$$\frac{L_f}{\sin(\theta_1) \cos(\beta) - \sin(\beta) \cos(\theta_1)} = \frac{R}{\cos(\theta_1)} \quad (3-27)$$

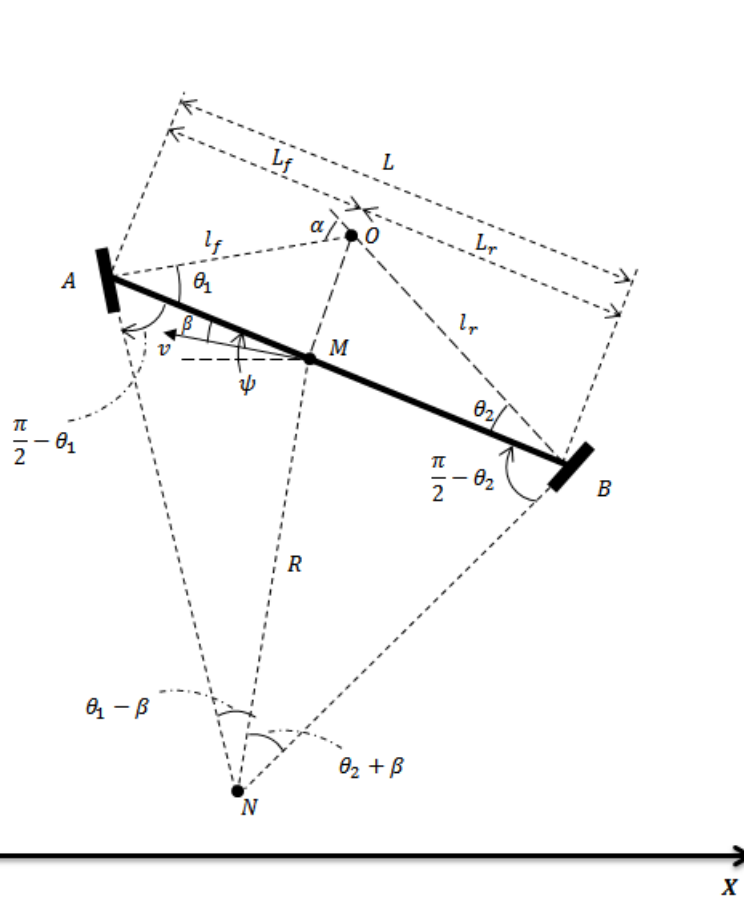


Figure 3-11: Kinematic model

And, applying sine rule to the triangle 'NMB',

$$\frac{L_r}{\sin(\theta_2 + \beta)} = \frac{R}{\sin(\frac{\pi}{2} - \theta_2)} \quad (3-28)$$

$$\frac{L_r}{\sin(\theta_2)\cos(\beta) + \sin(\beta)\cos(\theta_2)} = \frac{R}{\cos(\theta_2)} \quad (3-29)$$

multiplying both sides of Equation 3-27 by $\frac{\cos(\theta_1)}{L_f}$ and Equation 3-29 by $\frac{\cos(\theta_2)}{L_r}$, we get:

$$\tan(\theta_1)\cos(\beta) - \sin(\beta) = \frac{L_f}{R} \quad (3-30)$$

$$\sin(\beta) + \tan(\theta_2)\cos(\beta) = \frac{L_r}{R} \quad (3-31)$$

Adding the above equations and rearranging gives:

$$R = \frac{L}{\cos(\beta) (\tan(\theta_1) + \tan(\theta_2))} \quad (3-32)$$

Now, the slip angle β can be calculated by multiplying Equation 11 by L_r and subtracting it

from Equation 3-31 multiplied by L_f :

$$\beta = \tan^{-1} \left(\frac{L_r \tan(\theta_1) - L_f \tan(\theta_2)}{L} \right) \quad (3-33)$$

The rate of change of orientation angle is also the angular velocity of the machine. Therefore we have:

$$\dot{\psi} = \frac{v}{R} \quad (3-34)$$

Using equation 13, $\dot{\psi}$ can be calculated as:

$$\dot{\psi} = \frac{v \cos(\beta)}{L} (\tan(\theta_1) + \tan(\theta_2)) \quad (3-35)$$

The overall equations of motion can be given by :

$$x_{k+1} = x_k + v_k T \cos(\psi_k - \beta) \quad (3-36)$$

$$y_{k+1} = y_k + v_k T \sin(\psi_k - \beta) \quad (3-37)$$

$$\psi_{k+1} = \psi_k + \frac{v_k T \cos(\beta)}{L} (\tan(\theta_1) + \tan(\theta_2)) \quad (3-38)$$

where L , θ_1 and θ_2 are given by:

$$L = \sqrt{l_f^2 + l_r^2 - 2l_f l_r \cos(\pi - \alpha)}$$

$$\theta_1 = \sin^{-1} \left(\frac{l_r \sin(\pi - \alpha)}{L} \right)$$

$$\theta_2 = \sin^{-1} \left(\frac{l_f \sin(\pi - \alpha)}{L} \right)$$

where α is the articulation angle. Now, the other two models can be modified as follows:

Front only steering machine

In this model, with the given length of the machine, and the rear articulation angle being $\theta_2 = 0$, the model can be modified as:

$$x_{k+1} = x_k + v_k T \cos(\psi_k - \theta_1) \quad (3-39)$$

$$y_{k+1} = y_k + v_k T \sin(\psi_k - \theta_1) \quad (3-40)$$

$$\psi_{k+1} = \psi_k + \frac{v_k T \sin(\theta_1)}{L} \quad (3-41)$$

Front and rear steering machine

In this type of machine model, with the given length of the machine, the equations become:

$$x_{k+1} = x_k + v_k T \cos(\psi_k - \beta) \quad (3-42)$$

$$y_{k+1} = y_k + v_k T \sin(\psi_k - \beta) \quad (3-43)$$

$$\psi_{k+1} = \psi_k + \frac{v_k T \cos(\beta)}{L} (\tan(\theta_1) + \tan(\theta_2)) \quad (3-44)$$

where L, θ_1 and θ_2 are given by:

$$\theta_1 = \sin^{-1} \left(\frac{l_r \sin(\pi - \alpha)}{L} \right)$$

$$\theta_2 = \sin^{-1} \left(\frac{l_f \sin(\pi - \alpha)}{L} \right)$$

and $l_r = l_f = L/2$.

Kalman filters and State Estimation

4-1 Kalman filters for state and parameter estimation

A Kalman filter estimates the state of a noisy linear dynamic system by noisy measurements that could be linear related to the systems state. If the corrupting noise is independent, white and normal distributed with a zero mean; the KF will be a statistically optimal estimator with respect to any reasonable quadratic function of estimation error.

4-1-1 Linear Kalman Filters

The original KF assumes the underlying dynamic system to evolve in a linear manner and is for that particular reason commonly referred to as the linear Kalman filter (LKF).

Algorithm

A Kalman filter could be divided into two distinct phases. In the first phase, the prediction phase, the KF estimates the current state of the system based on the previous state using a given model of the system. This estimation is called the a priori state estimate since it is an estimate prior the observation of the system state. The latter is done in the second phase, the correction phase, where the current state is observed through sensor measurements. The observations are then combined with the a priori state estimate to form the a posteriori state estimate - an improved state estimation of the true system state.

Prediction Equations

Looking at the prediction phase, the a priori state estimate vector $\hat{x}_{k|k-1}$ and the a priori estimate error covariance matrix $P_{k|k-1}$ is given by:

$$\hat{x}_{k|k-1} = F_k \hat{x}_{k-1|k-1} + G_k u_k, \quad (4-1)$$

$$P_{k|k-1} = F_k P_{k-1|k-1} F_k^T + G_k \Gamma_k G_k^T + Q_k \quad (4-2)$$

In this phase the KF essentially drives the state forward in accordance with the system model and input model matrices represented by F_k and G_k , respectively. Through the covariance matrices Γ_k and Q_k , the KF is given knowledge about the noise corrupting the system state. Consequently the KF utilizes this knowledge to, with the estimate error covariance matrix, reflect the uncertainty of the a priori state estimate.

Correction Equations

The correction phase begins with calculating the innovation \tilde{y}_k reflecting the difference between the actual observation z_k and the predicted observation

$$\tilde{y}_k = z_k - H_k \hat{x}_{k|k-1} \quad (4-3)$$

and where the innovation covariance is given by

$$S_k = H_k P_{k|k-1} H_k^T + R_k \quad (4-4)$$

The Kalman gain K_k is a factor determining the extent of the innovation accounted for when calculating the a posteriori state estimate. The factor is determined by the relative uncertainty between the a priori state estimate and the innovation.

$$K_k = P_{k|k-1} H_k^T S_k^{-1} \quad (4-5)$$

$$= P_{k|k-1} H_k^T (H_k P_{k|k-1} H_k^T + R_k)^{-1} \quad (4-6)$$

Lastly the a posteriori state estimate $\hat{x}_{k|k}$, where the predicted state is corrected by the knowledge obtained from the observation, and the a posteriori estimate error covariance $P_{k|k}$ are calculated by:

$$\hat{x}_{k|k} = \hat{x}_{k|k-1} + K_k \tilde{y}_k \quad (4-7)$$

$$P_{k|k} = (I - K_k H_k) P_{k|k-1} \quad (4-8)$$

which completes the KF.

Kalman Filter is an optimal filter for estimating a linear system. Due to its simplicity, it has found its usage in numerous practical applications. However, many real-world systems are nonlinear in nature. In order to deal with nonlinearities, many extensions have been developed over the kalman filter. Here, Extended Kalman filter is described where it accounts for nonlinearities by linearizing the system about its last-known best estimate with the assumption that the error incurred by neglecting the higher-order terms is small in comparison to the first-order terms.

4-1-2 Extended Kalman filter

The Extended Kalman Filter (EKF) is an extension to the original KF to allow for its use on non-linear systems. The EKF uses a Taylor series approximation to linearize the state equations about the operating point. This linearization is made implicit within the filter by calculation of the Jacobian and Hessian matrices that represent the derivatives of the state and measurement transition matrices. A full derivation of the equations is not provided here, but can be found in [16]. Given the dynamics model and the measurement model,

$$x_k = f(x_{k-1}, u_k; \psi_k) + w_{k-1} \quad (4-9)$$

$$z_k = h(x_k; v_k) \quad (4-10)$$

where w_{k-1} and v_k are the process and observation noises which are both assumed to be zero mean multivariate Gaussian noises with covariance Q_k and R_k respectively. The function $f(\cdot)$ can directly be used by the EKF to compute the a priori state estimate

$$\hat{x}_{k|k-1} = f(\hat{x}_{k-1|k-1}, u_k) \quad (4-11)$$

$$(4-12)$$

However, it is not possible to apply $f(\cdot)$ directly to the computations of the a priori estimate error covariance. To deal with this problem the EKF linearizes $f(\cdot)$ around the a posteriori state estimate $\hat{x}_{k-1|k-1}$ of the previous time instance in accordance with

$$F_k = \left. \frac{\partial f}{\partial x} \right|_{\hat{x}_{k-1|k-1}} \quad (4-13)$$

$$G_k = \left. \frac{\partial f}{\partial u} \right|_{\hat{x}_{k-1|k-1}} \quad (4-14)$$

where the Jacobian matrices F_k and G_k contains the first-order partial derivatives of $f(\dots)$ with respect to the state x and input u vectors, respectively. The prediction phase is completed by calculating the a priori estimate error covariance

$$P_{k|k-1} = F_k P_{k-1|k-1} F_k^T + G_k \Gamma_k G_k^T + Q_k \quad (4-15)$$

Similar to the case of $f(\cdot)$ the function $h(\cdot)$ is directly applied to the a priori state estimate in the purpose of calculating the innovation

$$\tilde{y}_k = z_k - h(\hat{x}_{k|k-1}) \quad (4-16)$$

Again, in order to utilize $h(\cdot)$ in the remaining equations it needs to be linearized. This time the linearization takes place around the a priori state estimate $\hat{x}_{k|k-1}$ as started by

$$H_k = \left. \frac{\partial h}{\partial x} \right|_{\hat{x}_{k|k-1}} \quad (4-17)$$

$$(4-18)$$

where H_k is the the Jacobian matrix of $h(\dots)$ with respect to the state x . Finally the correction phase is completed by

$$K_k = P_{k|k-1} H_k^T (H_k P_{k|k-1} H_k^T + R_k)^{-1} \quad (4-19)$$

$$\hat{x}_{k|k} = \hat{x}_{k|k-1} + K_k \tilde{y}_k \quad (4-20)$$

$$P_{k|k} = (I - K_k H_k) P_{k|k-1} \quad (4-21)$$

which completes the EKF as well.

4-2 Model and Filter Validation

In this section, the filter and the machine model developed in the previous chapter is validated. It is assumed that the only information obtained from the GPS is position and velocity of the machine. With the help of an EKF the other states are estimated. Since the model developed in the previous chapter also has unknown parameters which are used to calculate the states, the same filter is also used for parameter estimation. The parameters are considered as additional states and augmented with the state equations. The augmented state equations are given by:

$$z_{k+1} = \begin{bmatrix} x_{k+1} \\ \theta_{k+1} \end{bmatrix} = \begin{bmatrix} f(x_k, u_k, \theta_k) \\ \theta_k \end{bmatrix} \quad (4-22)$$

where, x_{k+1} are the states and θ_k are the parameters to be estimated. Now, the states are defined in the following ways for pointmass and machine model:

Point mass filter

$$z_{k+1} = \begin{bmatrix} x_{k+1} \\ y_{k+1} \\ v_{k+1} \\ \theta_{k+1} \\ acc_{k+1} \end{bmatrix} = \begin{bmatrix} x_k + v_k T \cos(\theta_k) \\ y_k + v_k T \sin(\theta_k) \\ v_k + T acc_k \\ \theta_k \\ acc_k \end{bmatrix} \quad (4-23)$$

Machine Model

$$z_{k+1} = \begin{bmatrix} x_{k+1} \\ y_{k+1} \\ \psi_{k+1} \\ \theta_{1_{k+1}} \\ \theta_{2_{k+1}} \\ L_{k+1} \\ \beta_{k+1} \\ \alpha_{k+1} \end{bmatrix} = \begin{bmatrix} x_k + v_k T \cos(\psi_k - \beta) \\ y_k + v_k T \sin(\psi_k - \beta) \\ \psi_k + \frac{v_k T \cos(\beta)}{L} (\tan(\theta_{1_k}) + \tan(\theta_{2_k})) \\ \sin^{-1} \left(\frac{l_r \sin(\pi - \alpha_k)}{L} \right) \\ \sin^{-1} \left(\frac{l_f \sin(\pi - \alpha_k)}{L} \right) \\ \sqrt{l_f^2 + l_r^2 - 2l_f l_r \cos(\pi - \alpha_k)} \\ \tan^{-1} \left(\frac{L_r \tan(\theta_{1_k}) - L_f \tan(\theta_{2_k})}{L} \right) \\ \alpha_k \end{bmatrix} \quad (4-24)$$

The process and measurement covariance matrices Q and R , also act as the tuning matrices of the filter. The starting values for the tuning matrices were assumed to be diagonal matrices with diagonal elements as the standard deviation of the noise present in the GPS signals. So, for R we have,

$$R = \begin{bmatrix} \sigma_x & 0 & 0 \\ 0 & \sigma_y & 0 \\ 0 & 0 & \sigma_v \end{bmatrix} \quad (4-25)$$

After a number of simulations, the following values of Q and R gave desirable results.

$$R = \begin{bmatrix} 3.7334e-09 & 0 & 0 \\ 0 & 3.7334e-09 & 0 \\ 0 & 0 & 0.23 \end{bmatrix} \quad (4-26)$$

$$Q = \begin{bmatrix} 10^{-6} & 0 & 0 & 0 & 0 & 0 & 0 & 0 & 0 & 0 \\ 0 & 10^{-6} & 0 & 0 & 0 & 0 & 0 & 0 & 0 & 0 \\ 0 & 0 & 10^{-5} & 0 & 0 & 0 & 0 & 0 & 0 & 0 \\ 0 & 0 & 0 & 10^{-4} & 0 & 0 & 0 & 0 & 0 & 0 \\ 0 & 0 & 0 & 0 & 10^{-6} & 0 & 0 & 0 & 0 & 0 \\ 0 & 0 & 0 & 0 & 0 & 10^{-5} & 0 & 0 & 0 & 0 \\ 0 & 0 & 0 & 0 & 0 & 0 & 10^{-6} & 0 & 0 & 0 \\ 0 & 0 & 0 & 0 & 0 & 0 & 0 & 10^{-6} & 0 & 0 \\ 0 & 0 & 0 & 0 & 0 & 0 & 0 & 0 & 10^{-5} & 0 \\ 0 & 0 & 0 & 0 & 0 & 0 & 0 & 0 & 0 & 10^{-6} \end{bmatrix} \quad (4-27)$$

One of the essential aspect of the full kinematic model previously derived is the machine heading. The validity of the model is thereby possible to verify by comparing the heading measured by the GPS with the value obtained from the model. Also, along with the position and velocity, heading is the only other parameter obtained from the GPS. Hence the heading can be compared with the real heading obtained from GPS. In addition, the filtered position is also compared with the true GPS position. Sometimes, the filter behaves in favor of a single state on the cost of other states causing the filter to perform poorly. Hence its necessary to validate the crucial states (Position and Heading) of the system.

The plots clearly indicate that the filter is able to estimate the heading with good accuracy for both point mass model and machine model. Also, the position is being filtered with high accuracy described in the position error plot Figure 4-4 . With the validation of the filter, it can also be concluded that the combined machine model derived in th previous chapter reflects the behavior of the actual machine.

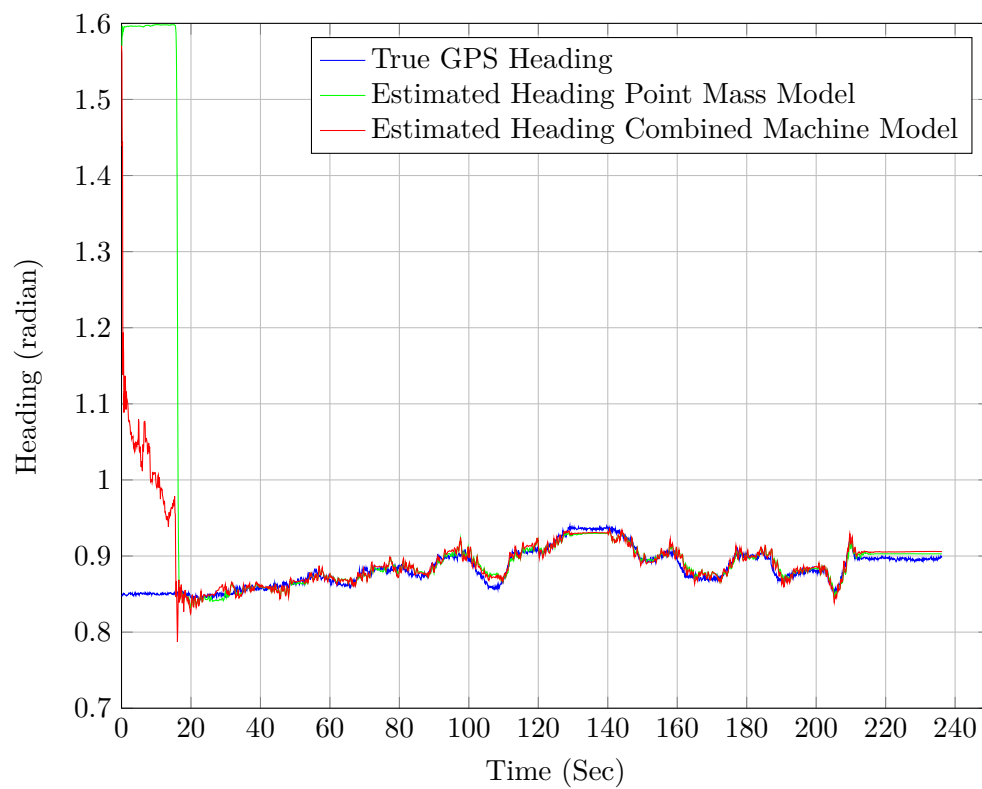


Figure 4-1: Estimated Heading angle comparison with True GPS Heading

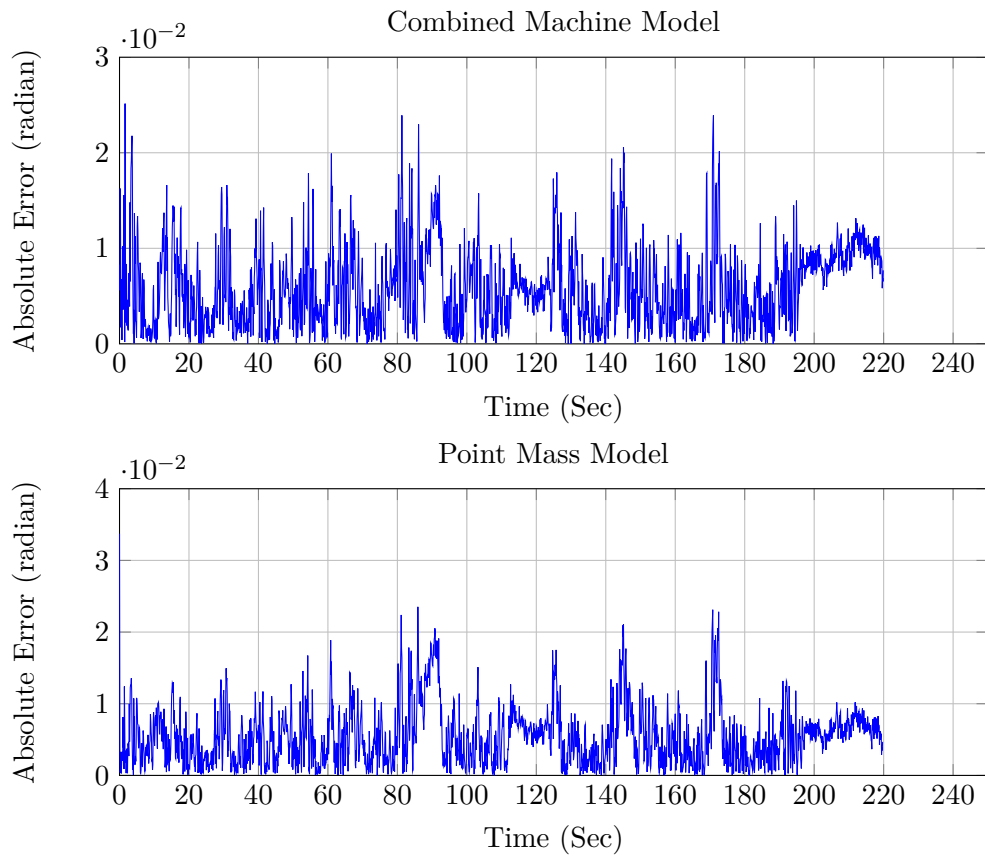


Figure 4-2: Absolute error between estimated and true heading

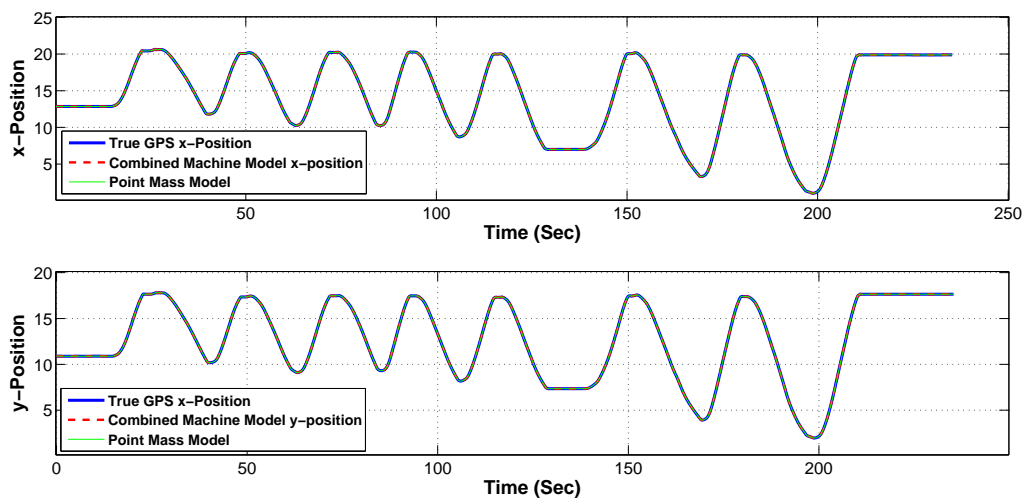


Figure 4-3: Filtered x-y Position vs true GPS x-y Position

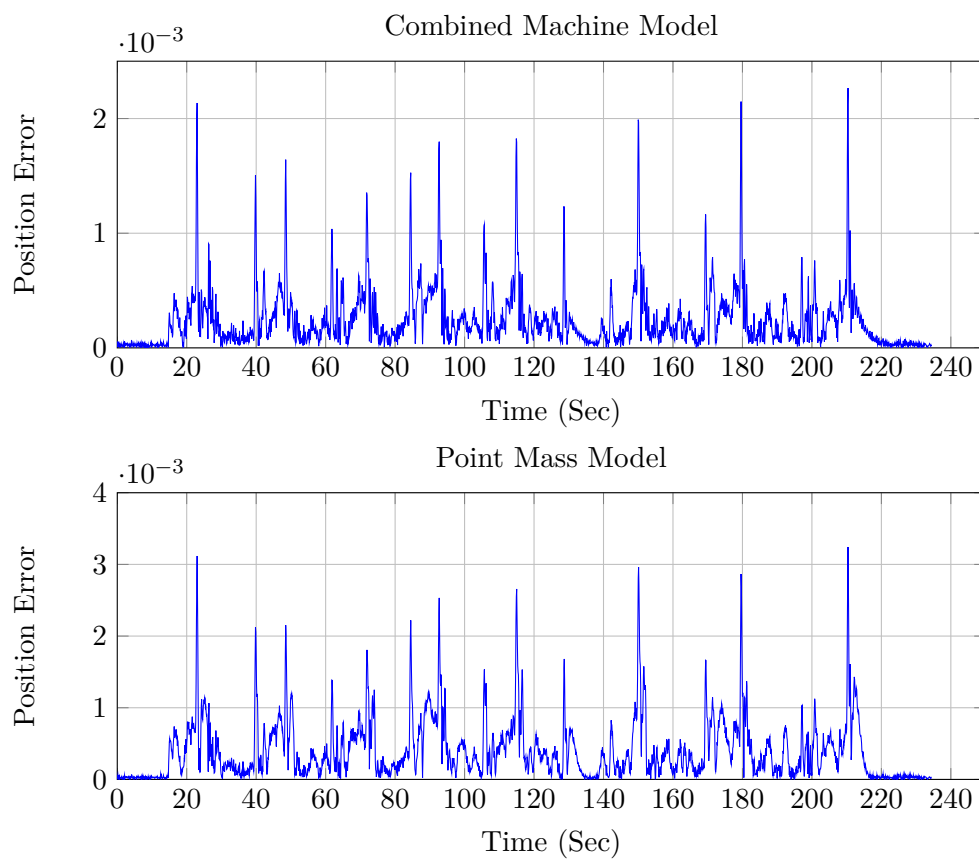


Figure 4-4: Absolute error between filtered and true GPS position

Threat Assessment System

5-1 Braking/Warning Model

In conventional Collision Avoidance System (CAS) functioning in today's cars/trucks, there are two zones defined for which the collision avoidance system performs two different functions.

- **Warning Zone:** This is the region, where the system anticipates a risk of collision and hence issues warning to the driver using some type of driver interface.
- **Braking zone:** If the driver fails to react to the warnings, and a machine/obstacle is detected in the braking zone, the machine is brought to a complete stop without the driver's intervention.

The same technique is utilized for this project. The two zones are determined by defining two prediction horizons for which the machine's position are calculated.

5-1-1 Warning/Braking Model

An effective CAS depends on many factors. Basically the system needs to reliably be able to detect surrounding objects, take decisions on when to warn, and finally issue the warnings to the driver using a human machine interface. The timing of a CAS alarm is fundamental to the functionality of the complete system. The algorithm used by CAS which results in this alarm timing is usually based on objective assumptions of a driver's response when required to brake, along with the physical characteristics of the vehicle in its stopping ability. For example, a CAS under development at Honda calculates the braking distance based on velocity, relative velocity and deceleration of the two vehicles [17]. Whenever the real distance between the following and the leading vehicle is less than the braking critical distance calculated by the algorithm, the CAS sounds its warning. Basically, two driver behavior parameters are critical in determining a driver's stopping distance based on a collision warning [17]. The first is the reaction time which is the time it takes the driver to understand the situation and apply

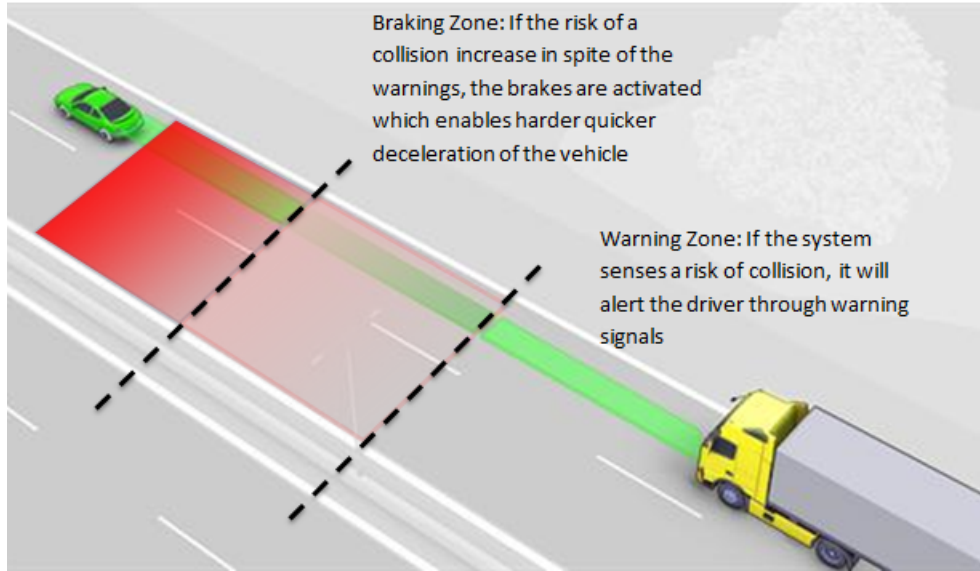


Figure 5-1: Conventional CAS utilized in Trucks and Passenger cars consisting of two regions: Braking and Warning region

the brakes in addition to a possible system delay to execute the command. The second parameter is the acceleration the driver applies. In order to calculate the appropriate warning time, a warning model which is widely recognized [18],[19] is used. According to the models, the stopping distance which the driver needs to bring the vehicle to a complete stop when receiving a warning is

$$d_{stop} = t_w v_w - \frac{v_w^2}{2a_r}$$

where t_w is the sum of the driver and brake system reaction time, a_r is the deceleration the driver responds applies to the warning, v_w is the vehicle speed at the time the warning is issued. Based on this model, it is possible to decide if a crash will occur and what the collision velocity v_c would be for given velocity and warning timing if t_w and a_r are known. Hence the important issue is to calculate the warning time t_w .

t_w is dependent two variables, the driver's reaction time and the brake system reaction time. It is assumed that the desired braking acceleration is constant and reached instantly when applying the brakes. The driver's reaction time is a variable which varies from driver to driver. There has been a lot of analysis performed on driver's reaction time [18][20], some standard organizations have even established norms (2.5 secs in the United states and 2.0 sec in Europe). In [21] it is stated that 85% of all drivers are able to react to a warning within 1.18 seconds whereas in [18], a reaction time of 1.12 was found to be appropriate.

Based on the above two analysis, a reaction time of 1.15 secs was selected for the warning model. The driver braking response is a factor which varies for different scenarios and also depends on the machine under consideration. It is assumed that there is no rise time during the braking period. Also, the braking response for construction machines will be lower due to their low operating speed. For this project it is assumed that the driver decelerates the machine at the rate of $-3.5m/s^2$.

Parameter	"Too early"	Recommended	"Too late"
Assumed reaction time	1.52 sec	1.18 sec	1.18 sec

Figure 5-2: Reaction time according to [21]

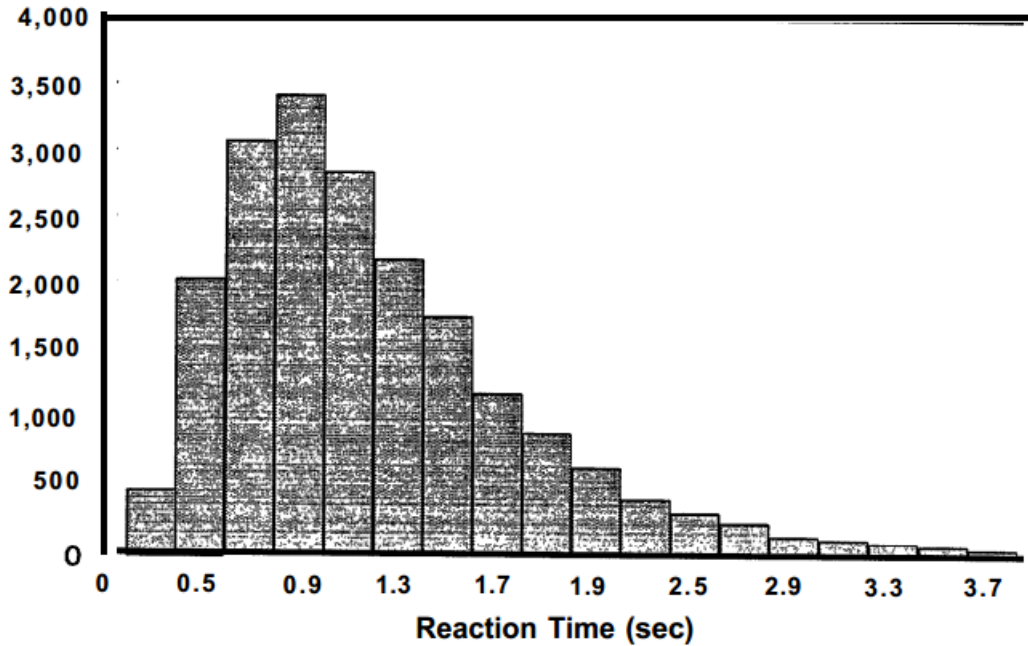


Figure 5-3: Lognormal Distribution of Driver Braking Reaction Times (Histogram at 0.2 Second Intervals) [18]

The two regions, warning and braking regions are defined as T_{warn} and T_{brake} . The idea is to calculate the predicted position every time step up to T_{warn} and T_{brake} and to warn the driver when an obstacle is detected in the warning region, and brake actively with full potential when an obstacle is detected in the braking region. Therefore, the final equations for calculating the two prediction horizons T_{warn} and T_{brake} are :

$$T_{warn} = \frac{v_w}{a_r} + t_{react} \quad (5-1)$$

$$T_{brake} = \frac{v_b}{a_{max}} \quad (5-2)$$

where, t_{react} is the reaction time considered as 1.15 sec, v_w is the velocity of the machine when an obstacle/machine is detected in the warning zone, a_r assumed acceleration with which the driver reacts for the warnings issued, v_b is the velocity of the machine when an obstacle/machine is detected in the braking zone and a_{max} the maximum acceleration with which the machine decelerates to bring the machine to a complete stop.

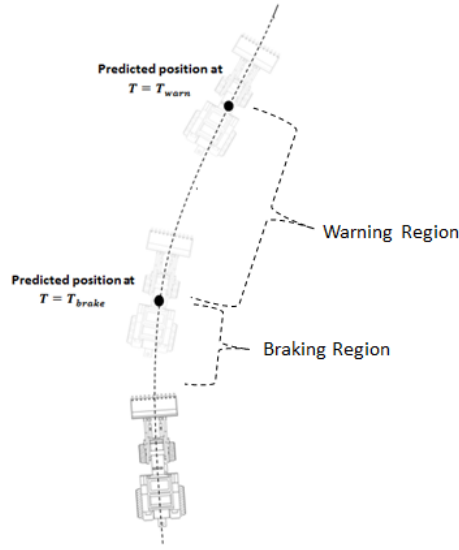


Figure 5-4: Visual representation of the two regions

5-2 Prediction Results

The prediction model that is utilized is described in (5-3) to (5-6). Two different trajectories were considered to validate the predictions one being more nonlinear than the other. The two trajectories considered are described in the plot Figure 5-5:

$$x_{k+1} = x_k + v_k T \cos(\psi_k - \beta) \quad (5-3)$$

$$y_{k+1} = y_k + v_k T \sin(\psi_k - \beta) \quad (5-4)$$

$$v_{k+1} = v_k + T acc_k \quad (5-5)$$

$$\psi_{k+1} = \psi_k + \frac{v_k T \cos(\beta)}{L} (\tan(\theta_{1_k}) + \tan(\theta_{2_k})) \quad (5-6)$$

These trajectories are obtained from recorded GPS measurements from the machines and are used as the input for the filter. Following results describes the error between the GPS measurements and the predicted position for the two prediction horizons. Results for each of the two trajectories are described for both prediction horizons, $t = t_{brake}$ and $t = t_{warn}$. The error for prediction horizon t_{brake} is usually less since a machine does not require much time to brake completely utilizing its full potential. Also, The predictions are calculated for both point mass model and the machine model and compared.

For Trajectory A

For trajectory A, the results obtained from point mass models are similar to the machine model with machine model performing marginally better than the point mass model. This can be attributed to linearity of the trajectory.

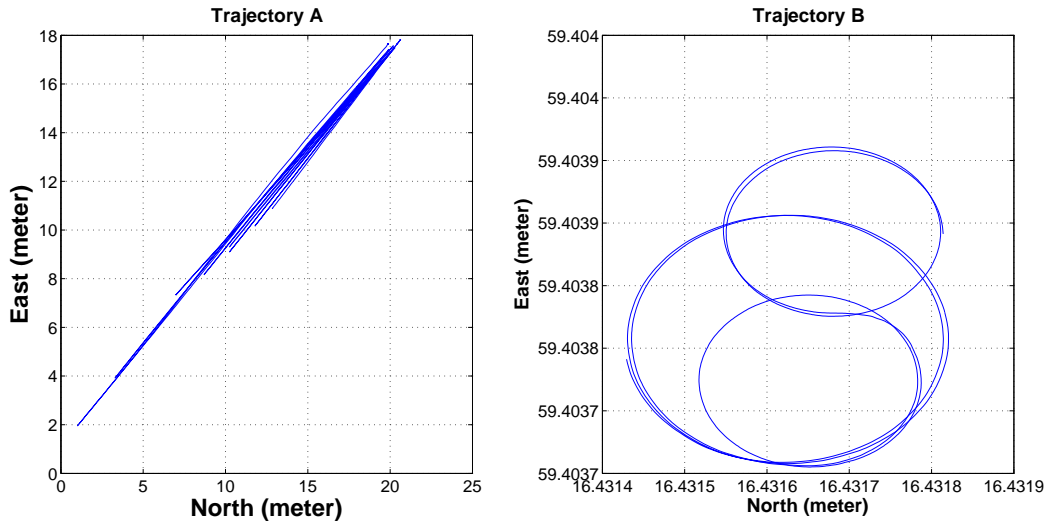


Figure 5-5: Real-Time Trajectories A and B on which the whole analysis has been conducted.

Model	RMS of Error
Point Mass Model	0.0520
Machine Model	0.0475

Table 5-1: RMS Position Error Comparison for $t = t_{brake}$

Model	RMS of Error
Point Mass Model	0.6619
Machine Model	0.6596

Table 5-2: RMS of Position Error Comparison for $t = t_{warn}$

For Trajectory B

Model	RMS of Error
Point Mass Model	0.1179
Machine Model	0.1046

Table 5-3: RMS Position Error Comparison for $t = t_{brake}$

Type of Trajectory	RMS of Error
Point Mass Model	1.0383
Machine Model	0.8057

Table 5-4: RMS Position Error Comparison for $t = t_{warn}$

In this trajectory, the path contains more non-linearity which causes the point mass model to perform poor. The machine model, which reflects the behaviors of the actual machine is able to determine the actual dynamics involved and hence performs better than the point mass

model when the machine has to follow a non-linear trajectory. A conclusion can be made that the point mass models fails to capture the dynamics of the machine and hence is not a reliable model for calculating predictions. Point mass models have an advantage when it comes to simplicity, but a trajectory of a machine cannot be anticipated and hence a system which can perform in both kind of trajectories has to be utilized. The further analysis in the report is based on the machine model.

5-2-1 Prediction using Iterative Extended Kalman Filter (EKF)

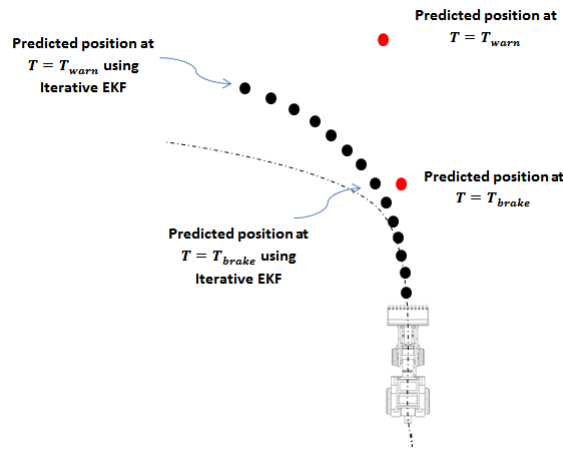


Figure 5-6: Iterative EKF calculates the new predictions for a horizon of 0.1 iterated till $t = t_{warn}$ and $t = t_{brake}$

The prediction model used for the analysis so far calculates the future positions based on the model described in (5-3) to (5-6), where T varies every sample according to the calculated T_{warn} and T_{brake} . There exists another technique for calculating the predictions. The technique used in the analysis so far faces a serious issue while addressing non-linear trajectories. When the prediction horizon is large, the model fails to anticipate the non linearities and hence causes the position error to be large. This problem can also arise when the machine makes abrupt changes in its trajectory. The issue can be described in the Figure 5-6. The predictions are calculated based on the present states alone which causes the large errors in the position when the prediction horizon is large. In order to deal with this problem an iterative EKF is utilized in which the filter is iterated upto the calculated prediction horizon. Since the input measurements are not available for the future estimation calculations, the measurements matrix is considered as zero and only the time update is performed. The time update is performed for The results are shown in the following figures.

Trajectory B	RMS of Error
$t = t_{brake}$	0.1540
$t = t_{warn}$	0.5902

Table 5-5: RMS of position error for Trajectory B using Iterative EKF method

Algorithm 1 Calculating Predictions Using Iterative Time Update of EKF

```

1: procedure ITER EKF
2:    $t_{samp} = \text{SmamplingTime}$ 
3:    $iter = t_{warn}/t_{samp}$ 
4:   for  $i=1: iter$  do
5:      $T=0.1$ 
6:      $z_{k+1} = \begin{bmatrix} x_k + v_k T \cos(\psi_k - \beta) \\ y_k + v_k T \sin(\psi_k - \beta) \\ \psi_k + \frac{v_k T \cos(\beta)}{L} (\tan(\theta_{1k}) + \tan(\theta_{2k})) \\ \sin^{-1} \left( \frac{l_r \sin(\pi - \alpha_k)}{L} \right) \\ \sin^{-1} \left( \frac{l_f \sin(\pi - \alpha_k)}{L} \right) \\ \sqrt{l_f^2 + l_r^2 - 2l_f l_r \cos(\pi - \alpha_k)} \\ \tan^{-1} \left( \frac{L_r \tan(\theta_{1k}) - L_f \tan(\theta_{2k})}{L} \right) \\ \alpha_k \end{bmatrix}$ 
7:   end for
8:   Return  $z_{k+1}$ 
9: end procedure

```

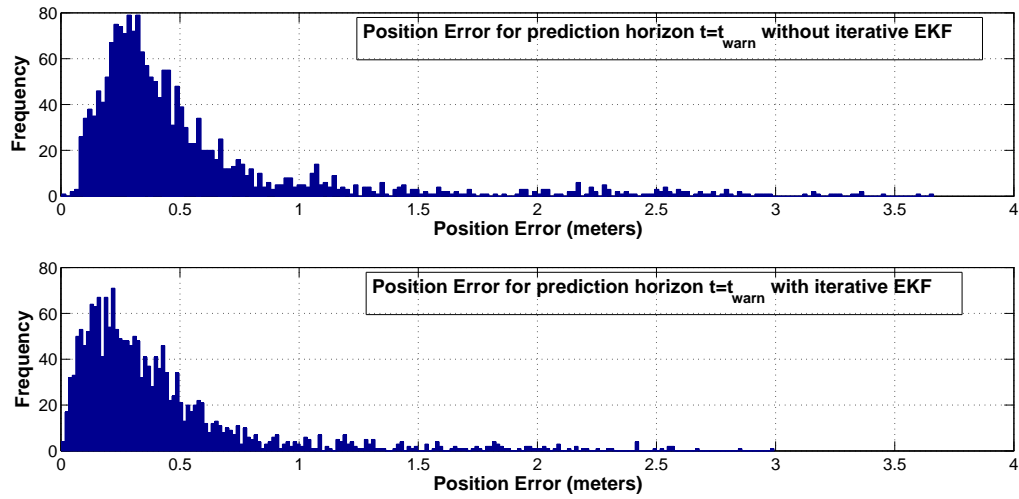


Figure 5-7: Histogram Comparison of position error calculated at prediction horizon $t = t_{warn}$ for trajectory B with and without Iterative EKF

The comparison is conducted for both trajectory A and B. Trajectory A being more linear produces more or less the same results for the type of models. Trajectory B on the other hand is more nonlinear hence providing a better idea on how the iterative EKF works better than the prediction model used in the previous analysis. The results describes the improvements achieved by the iterative EKF method over the normal prediction model especially for trajectory B.

The root mean square of the position error for $t = t_{warn}$ is reduced by 20%. A better understanding of the problem can be achieved by looking at the histogram plot. Apart from

the reduced RMS values, another important aspect which the iterative EKF accomplishes is the reduced frequency of position errors which are more than 1 meters Figure 5-7. The CAS becomes much more efficient when the position error of the predictions is less than 1 meters. This is a major advantage over the normal prediction method, since the normal method calculates predictions which are at instances more than 3 meters because of the reasons explained before Figure 5-6.

5-3 Combined Machine Model vs True Machine Model

The- combined machine model was developed in order to save the extra computational power caused while using the three different models individually but not on the cost of model performance. This section compares the results obtained from predictions calculated at $t = t_{warn}$ for the combined machine model and their original machine models. The system was investigated with two type of machines models, the waist steered machines and the front only steered machines. The results are described below:

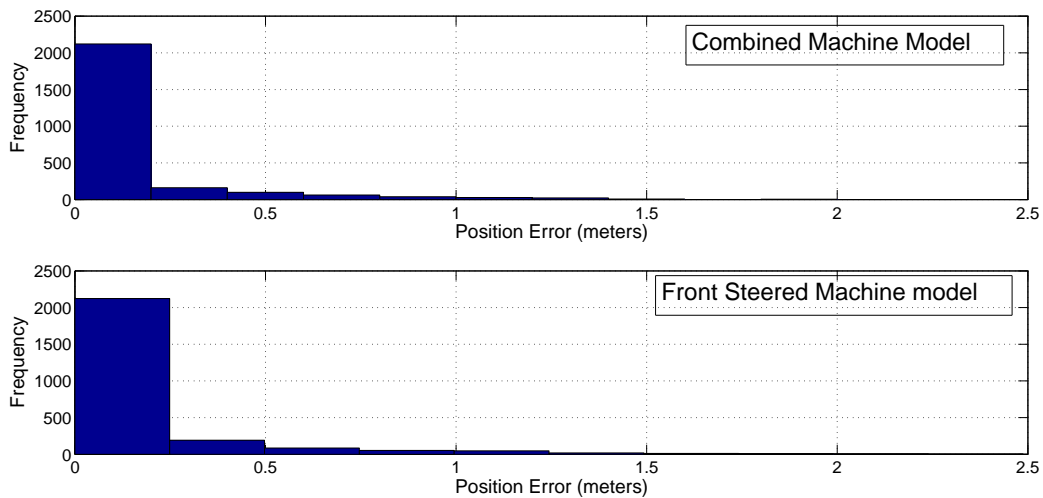


Figure 5-8: Histogram Comparison of position error calculated at prediction horizon of $t = t_{warn}$ (Front Steered Model)

Front Steered Machine	RMS of Error
Machine Model	0.2895
True Machine Model	0.3417

Table 5-6: RMS comparison of position error calculated at prediction horizon of $t = t_{warn}$ for Front steered machine

For both the cases the combined machine model reflects the behavior of the machine better than its actual model. This can be attributed to the fact that combined machine model is capable to capture more dynamics when compared to the front and waist steered machine. The performance would be similar if the true machine model is capable to capture the dynamics introduced in the combined machine model. But again, adding more dynamics to

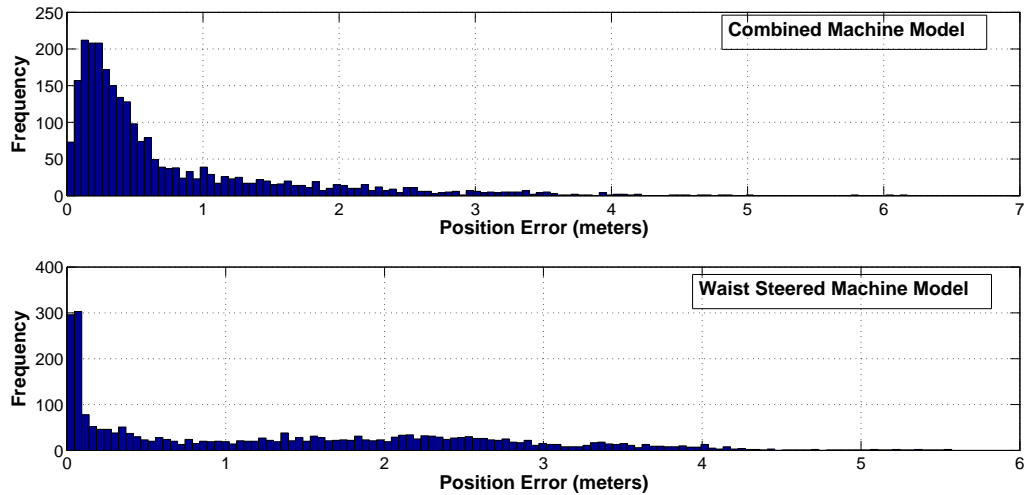


Figure 5-9: Histogram Comparison of position error calculated at prediction horizon of $t = t_{warn}$ (Waist Steered Model)

Front Steered Machine	RMS of Error
Machine Model	1.1075
True Machine Model	1.4630

Table 5-7: RMS comparison of position error calculated at prediction horizon of $t = t_{warn}$ for articulated steered machine

the true model and using them together in the system would increase the complexity and computational load of the overall system which is not desirable.

5-4 Fault Detection Based on Residual

For a collision warning system to be effective there are many requirements that need to be fulfilled. To start with, the system needs to reliably be able to detect surrounding objects, take decisions on when to warn, and finally issue the warn to the driver using a human machine interface. The importance of the timing of the warning has been pointed out in several publications [24]. The requirements on the warning timing can be expressed in two opposing requirements [24]:

- the warning should be early enough so that the driver can react and avoid the accident
- the warning should be late enough so that it does not trigger during normal operation conditions

If the first requirement is not fulfilled, the driver will not be able to avoid the accident. In this case, the collision might in best case be mitigated. If the second requirement is not fulfilled, the system will warn in situations where the operator perceives the warning as inappropriate

since he or she is in full control of the situation. This will cause irritation among the drivers and lead to miss-trust in the system. If possible, the drivers might actually turn the function off [26]. These consequences will result in either severely limited or no safety benefits.

Global Positioning System (GPS) measurements are sometimes corrupted with high level of noise. Hence, the predictions obtained are sometimes false. The idea is to switch of the warning system when the predictions obtained are false. In order to have such a system which could anticipate the false predictions, the prediction system was tested on real time data to check where the predictions have the largest error. It was found that every time the machine changes direction or has a abrupt change in the velocity, the predictions started to have large error.

This problem is solved using a moving horizon based residual approach. At every sample, the position is predicted at $T = 1$ and compared with the true GPS location. Whenever the error difference between the true GPS position and the prediction is more than a threshold value, the system stops issuing warnings. A moving horizon is set up each for the GPS inputs and for the predictions calculated. At time t the , the last T GPS measurements and predictions are known.

$$GPS = \begin{bmatrix} x(t-T) & x(t-T+1) & \cdots & x(t-1) & x(t) \\ y(t-T) & y(t-T+1) & \cdots & y(t-1) & y(t) \end{bmatrix} \quad (5-7)$$

$$P\hat{red}_{Pos} = \begin{bmatrix} \hat{x}(t-T) & \hat{x}(t-T+1) & \cdots & \hat{x}(t-1) & \hat{x}(t) \\ \hat{y}(t-T) & \hat{y}(t-T+1) & \cdots & \hat{y}(t-1) & \hat{y}(t) \end{bmatrix} \quad (5-8)$$

The window size is calculated by:

$$W_s = \frac{PredictionHorizon}{Samplingtime} \quad (5-9)$$

where the prediction horizon is a tuning parameter. The residual is given by:

$$Res = \sqrt{(\hat{x}(t-T) - x(t))^2 + (\hat{y}(t-T) - y(t))^2} \quad (5-10)$$

Based on this residual the divergence is anticipated and the warning system is switched of. The result is shown in Figure 5-11. The red lines indicate the instances when the algorithm anticipates the divergence. During these instances the warnings will be switched off.

This can be considered as one of the drawbacks of the system since, the warnings does not have a 100% operating region. These situations exist when the driver makes abnormal maneuvers or when the GPS is corrupted with significant noise level.

5-5 Collision Detection Algorithm

After the predictions are calculated for the two predictions horizons, the next step is to detect the possibility of a collision. In order to achieve that, the machines have to be represented in some form since, the GPS only provides the point mass location. There can be different ways of representing the machines given the length and breadth of the machine. Two of the most

Algorithm 2 Fault Detection Algorithm

```

1: procedure ERR DETECT
2:   Ph=Prediction Horizon
3:    $t_{samp} = SamplingTime$ 
4:    $T = Ph/t_{samp}$ 
5:    $GPS = zeros(2, T)$ 
6:    $Pred = zeros(2, T)$ 
7:    $GPS = \begin{bmatrix} x(t-T) & x(t-T+1) & \dots & x(t-1) & x(t) \\ y(t-T) & y(t-T+1) & \dots & y(t-1) & y(t) \end{bmatrix}$ 
8:    $Pred = \begin{bmatrix} \hat{x}(t-T) & \hat{x}(t-T+1) & \dots & \hat{x}(t-1) & \hat{x}(t) \\ \hat{y}(t-T) & \hat{y}(t-T+1) & \dots & \hat{y}(t-1) & \hat{y}(t) \end{bmatrix}$ 
9:    $err = \sqrt{(\hat{x}(t-T) - x(t))^2 + (\hat{y}(t-T) - y(t))^2}$ 
10:  for  $i=1:T$  do
11:     $GPS(:, i) = GPS(:, i+1)$ 
12:     $Pred(:, i) = Pred(:, i+1)$ 
13:  end for
14: end procedure

```

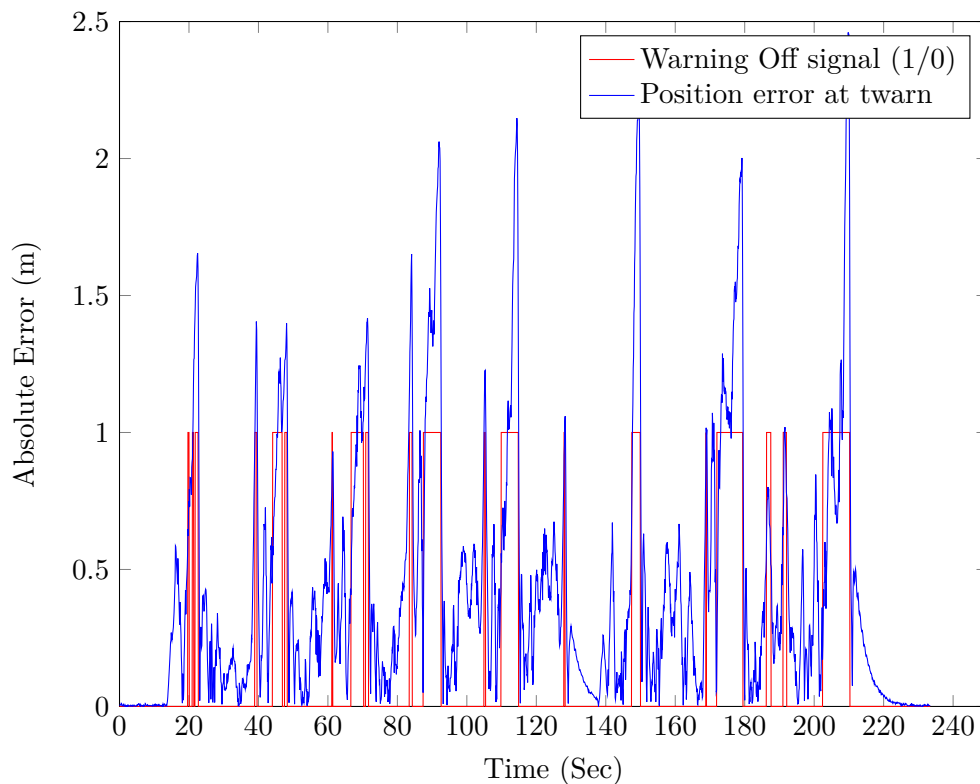


Figure 5-10: Warning off signals when Position error increases more than a threshold value (1 meter)

prominent ways of representing the machine is by circles and polygons. In many analysis for obstacle avoidance, the machine as well as the obstacles are represented as circles with

fixed radius [22], [8]. but in those applications, the system developed was a machine specific application. As discussed earlier, generalization is considered as one of the main factors of the project. Representing construction machines as circles lead to an additional problem. With increasing size of the machine, the circular representation adds on more ineffective space to the algorithm. This can be represented by the following figure :

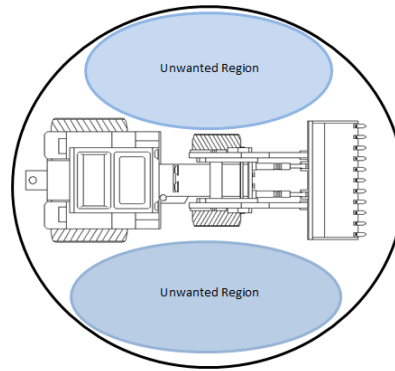


Figure 5-11: Problem using Circles for representing Machines and their predictions

To overcome this issue, the machines are represented as convex polygons. Given the length and the width of the machine, the convex polygons provides much more efficient way of representing the machines. Separating axis theorem is one of the widely used algorithms for collision detection [33]. It states the following:

- if two convex polygons are not intersecting, there exists a line that passes between them.
- such a line only exists if one of the sides of one of the polygons forms such a line

Basic Idea of Separating Axis Theoram

A test for non intersection of two convex objects is simply stated: If there exists a line for which the intervals of projection of the two objects onto that line do not intersect, then the objects are do not intersect. Such a line is called a separating line or, more commonly, a separating axis. The translation of a separating line is also a separating line, so it is sufficient to consider lines that contain the origin.

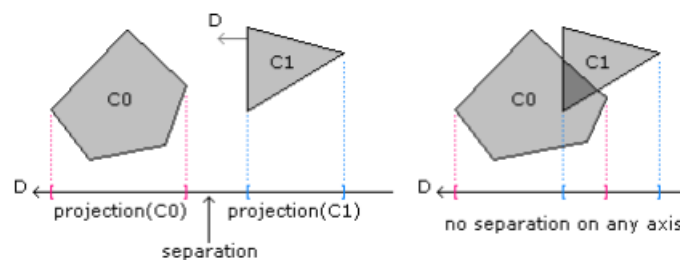


Figure 5-12: Separating Axis Theorem visual representation

For a pair of convex polyhedral in 3D, only a finite set of direction vectors needs to be considered for separation tests. That set includes the normal vectors to the faces of the polyhedra and vectors generated by a cross product of two edges, one from each polyhedron. The intuition is similar to that of convex polygons in 2D. If the two polyhedra are just touching with no inter penetration, then the contact is one of face-face, face-edge, face-vertex, edge-edge, edge-vertex, or vertex-vertex. In any of these cases, the algorithm would detect a collision.

Projection

The next concept that Separating Axis Theorem (SAT) uses is projection. Imagine that you have a light source whose rays are all parallel. If light is shown at an object, it will create a shadow on a surface. A shadow is a two dimensional projection of a three dimensional object. The projection of a two dimensional object is a one dimensional shadow.

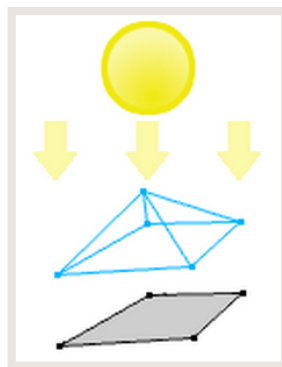


Figure 5-13: A 2-D projection of a 3-D Convex Polygon

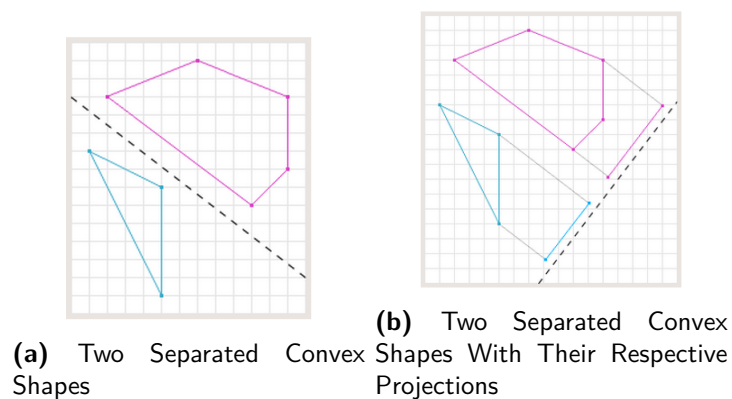


Figure 5-14: Non-Intersecting Polygons

No Intersection

If we choose the perpendicular line to the line separating the two shapes in Figure 5-14a, and project the shapes onto that line we can see that there is no overlap in their projections. A line where the projections (shadows) of the shapes do not overlap is called a separation axis. In Figure 5-14b the dark gray line is a separation axis and the respective colored lines are the projections of the shapes onto the separation axis. Notice in Figure 5-14b the projections are not overlapping, therefore according to SAT the shapes are not intersecting.

Intersection

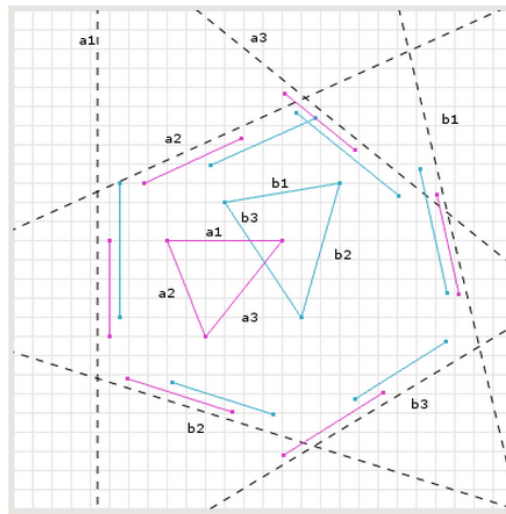


Figure 5-15: Two Intersecting Polygons

If, for all axes, the shape's projections overlap, then we can conclude that the shapes are intersecting. Figure 5-15 illustrates two convex shapes being tested on a number of axes. The projections of the shapes onto those axes all overlap, therefore we can conclude that the shapes are intersecting.

The host machines and the other machines and their predictions are represented as convex polygons. Hence the theorem explained above can be utilized in real time collision detection among the polygons. The plots Figure 5-16 to Figure 5-20 describes how the algorithm works in real time. During each time sample, every side of both the polygons are projected on four axes (4 sided convex polygons) and calculated if an overlap exists among the respective projections.

5-6 Plots

The following section describes the results obtained from different analysis performed in the thesis project. First, the position errors are plotted for the point mass model and combined machine model for trajectory A and B. It is followed by the position error obtained from the

iterative EKF method. After the analysis of the different plots, collision detection algorithm using SAT is described. Finally, a scenario is simulated for the Trajectory A , where the machine is simulated to collide with an stationary obstacle. The plots describe the different scenarios which can happen during real time implementation of the system.

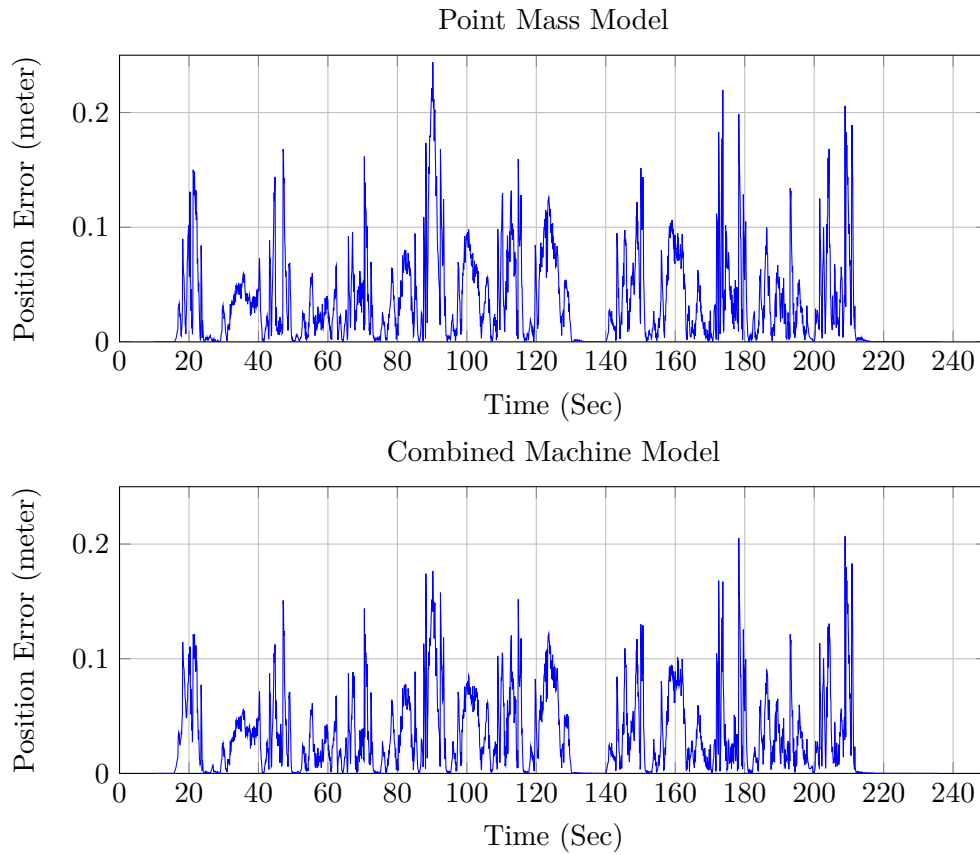


Figure 5-16: Trajectory A: Error plot for Point Mass and Machine Model, for a predicted horizon $t = t_{brake}$

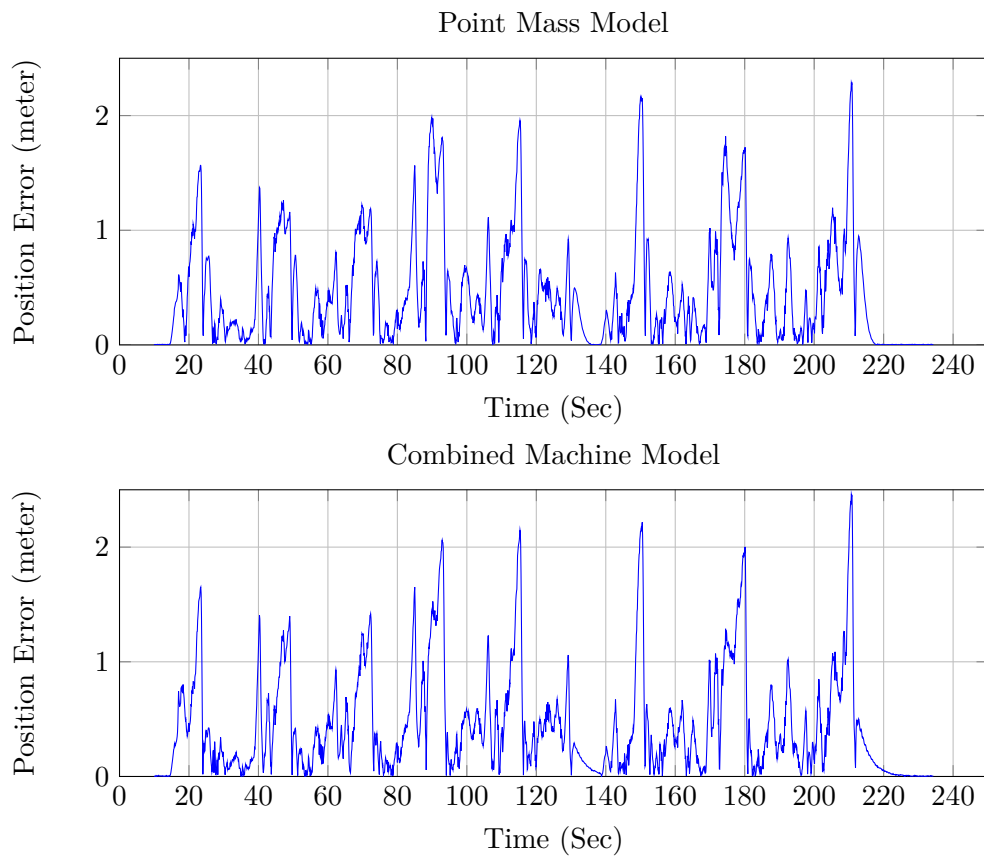


Figure 5-17: Trajectory A: Error plot for Point Mass and Machine Model, for a predicted horizon $t = t_{warn}$

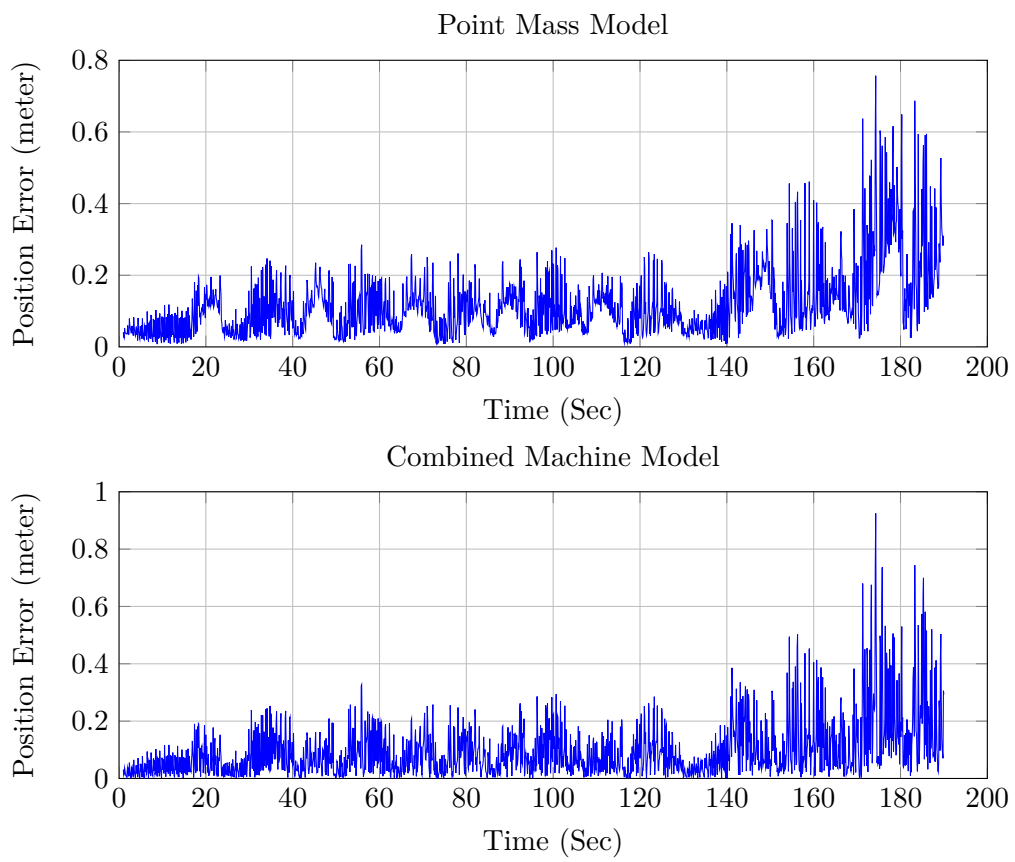


Figure 5-18: Trajectory B: Error plot for Point Mass and Machine Model, for a predicted horizon $t = t_{brake}$

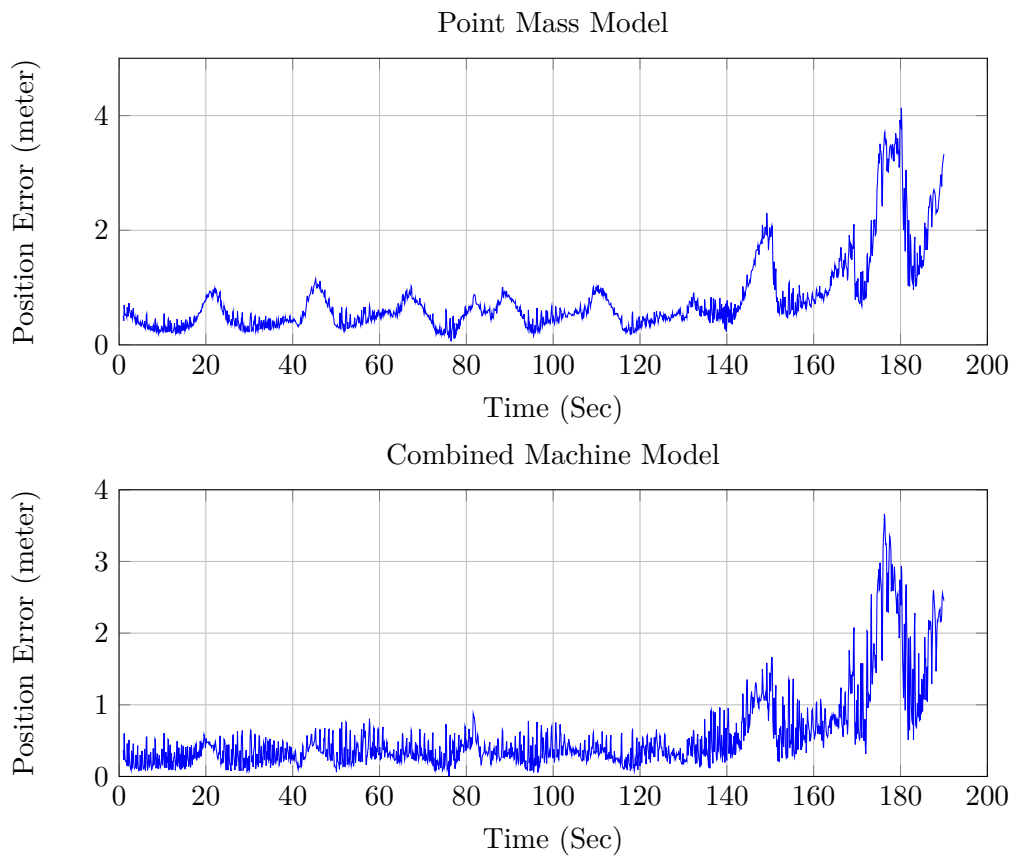


Figure 5-19: Trajectory B: Error plot for Point Mass and Machine Model, for a predicted horizon $t = t_{warn}$

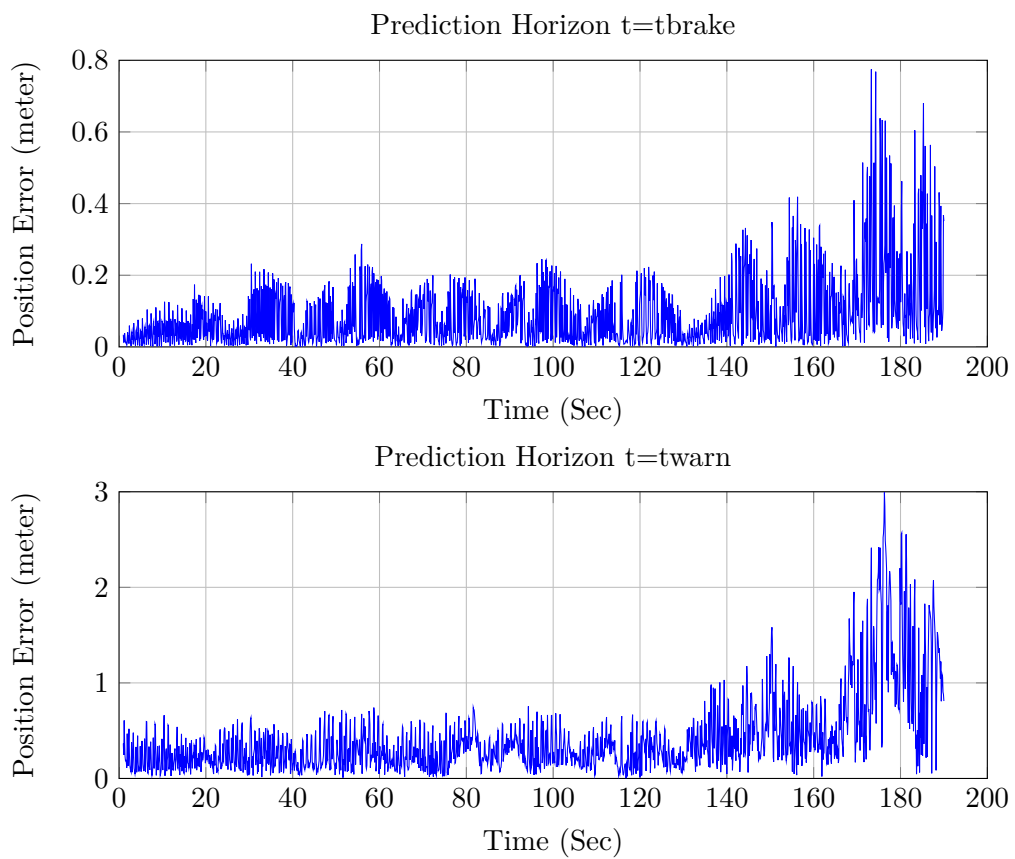


Figure 5-20: Trajectory B: Error Plot calculated using iterative EKF method for both predicted horizons $t = t_{warn}$ and $t = t_{brake}$

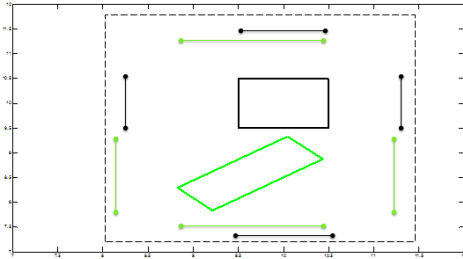


Figure 5-21: Collision not detected: The polygons 1 (black) and 2 (green) do not intersect each other. On the right and left part, the projections do not overlap each other

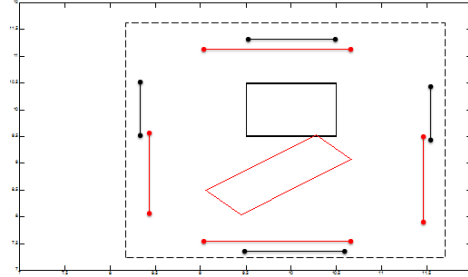


Figure 5-22: Collision detected: One side of the polygon 1 (black) intersects two sides of the polygon 2 (red). On all four sides, the projections overlap each other.

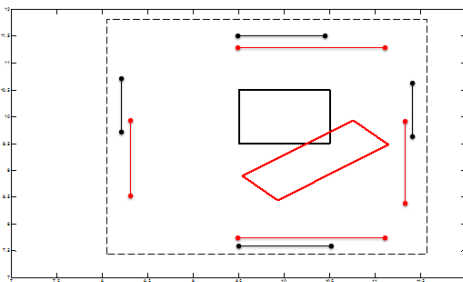


Figure 5-23: Collision detected: Two sides of the polygon 1 (black) intersects one side of the polygon 2 (red). On all four sides, the projections overlap each other.

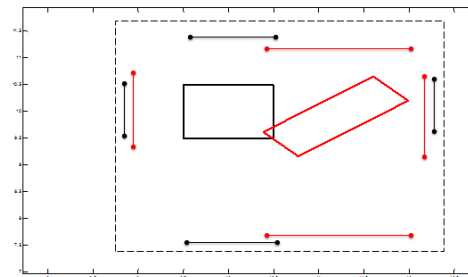


Figure 5-24: Collision detected: One side of the polygon 1 (black) intersects two sides of the polygon 2 (red). On all four sides, the projections overlap each other.

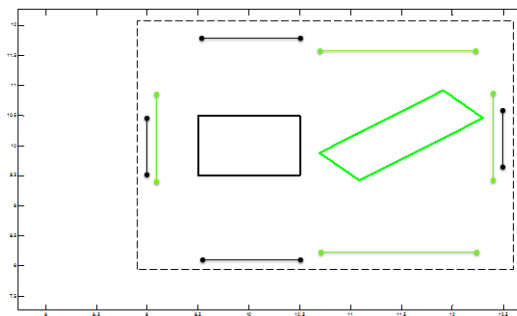


Figure 5-25: Collision not detected: The polygons 1 (black) and 2 (green) do not intersect each other. On the top and bottom, the projections do not overlap each other

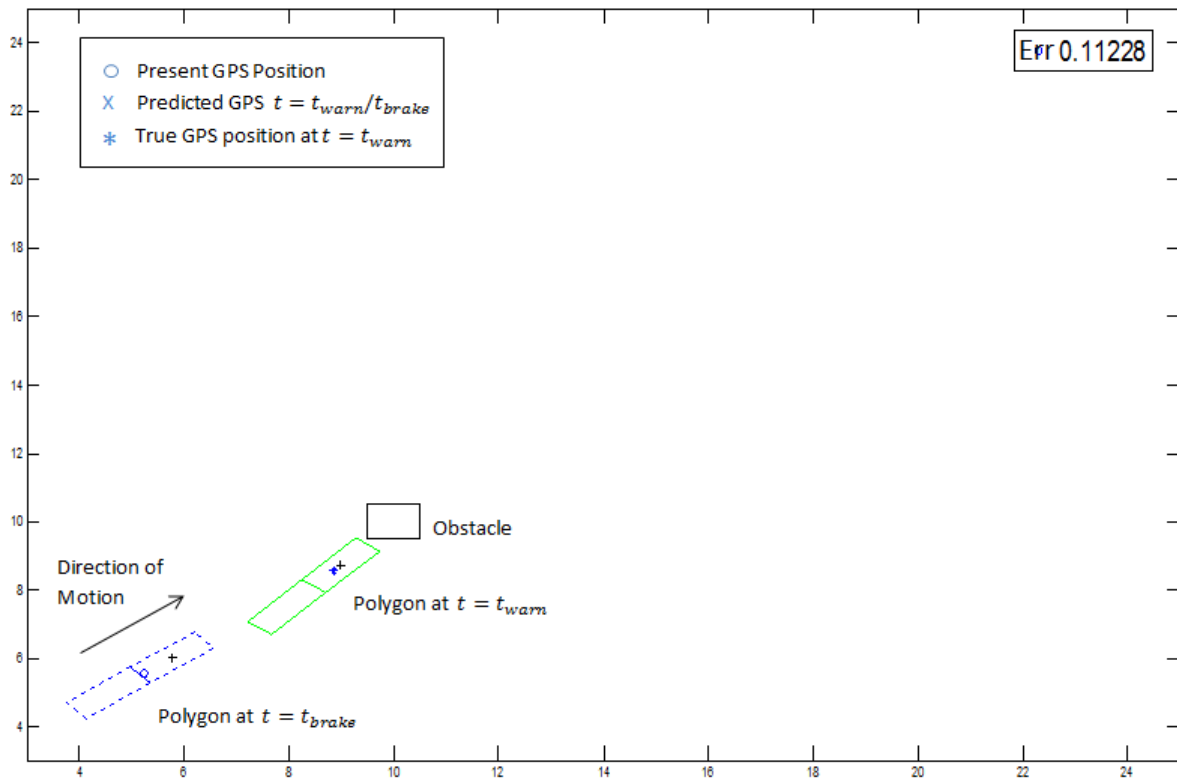


Figure 5-26: Plot describing a collision scenario of a waist steered machine with a stationary obstacle. Two parts of each of the polygon depicts the front and rear part of waist steered machine. In this scenario, the machine is simulated to collide with the obstacle. The position error at $t = t_{warn}$ is given at the top right of the plot which varies at every time sample.

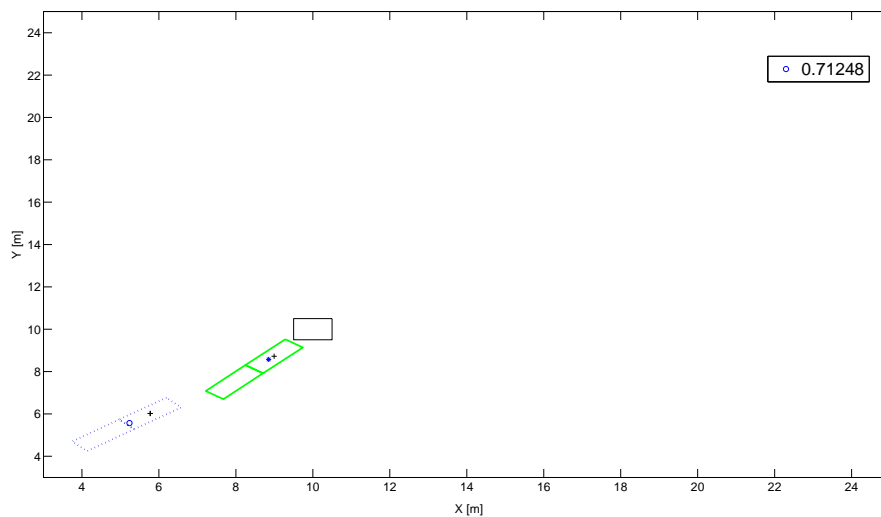


Figure 5-27: Polygon in Green for t_{warn} and in blue for t_{brake} indicates that there is no collision detected among the predicted position and obstacle.

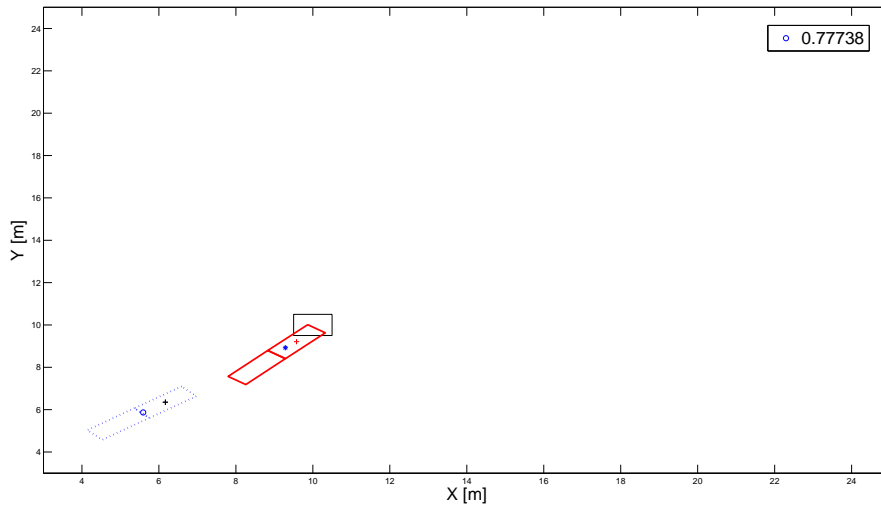


Figure 5-28: The polygon detects a collision and hence turns into red. At this moment, the system will warn the driver of a possible collision through Human Machine Interface (sound/light warnings)

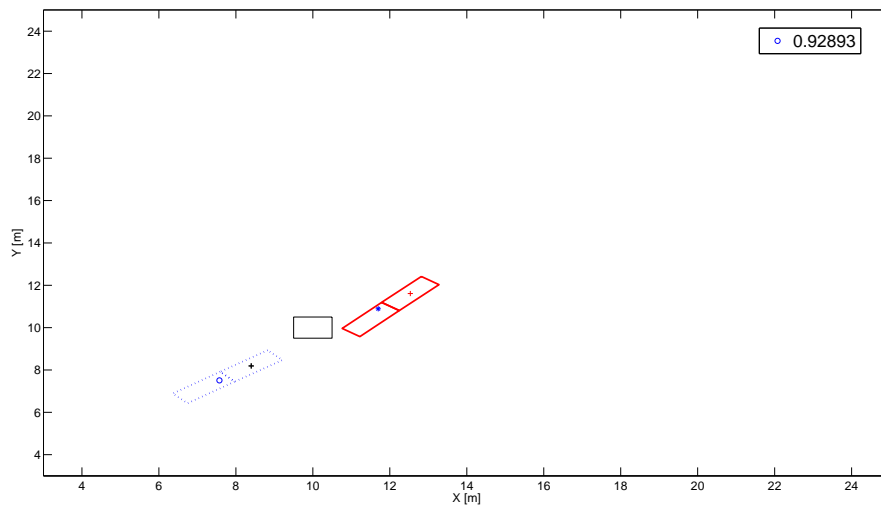


Figure 5-29: This is a scenario when the driver does not respond to the warnings. The polygon at $t = t_{warn}$ is still in red color and continues issuing warning because the algorithm still detects a collision between the position at $t = t_{warn}$ and $t = t_{brake}$. This is done by performing the collision detection algorithm for every time sample existing between $t = t_{warn}$ and $t = t_{brake}$.

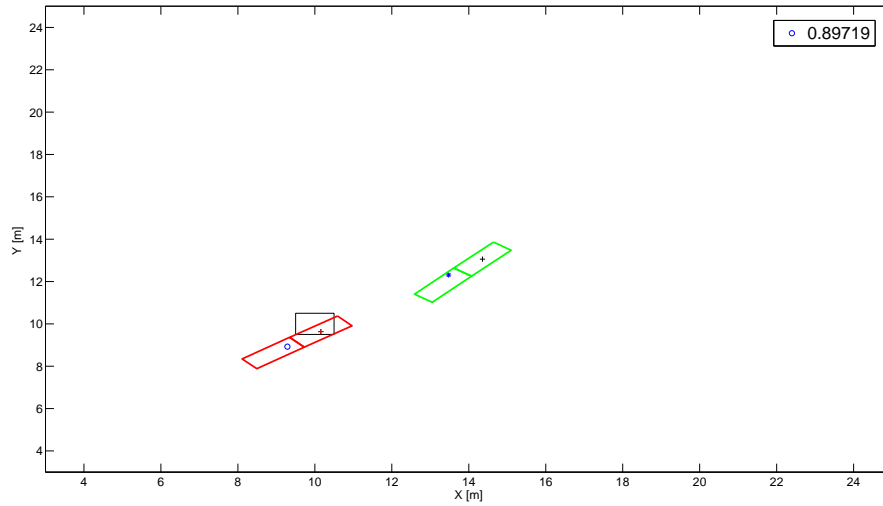


Figure 5-30: The obstacle's presence in the braking region turns the polygon to red color. As soon as the polygon detects a collision, the machine is brought to full stop by applying its maximum deceleration force

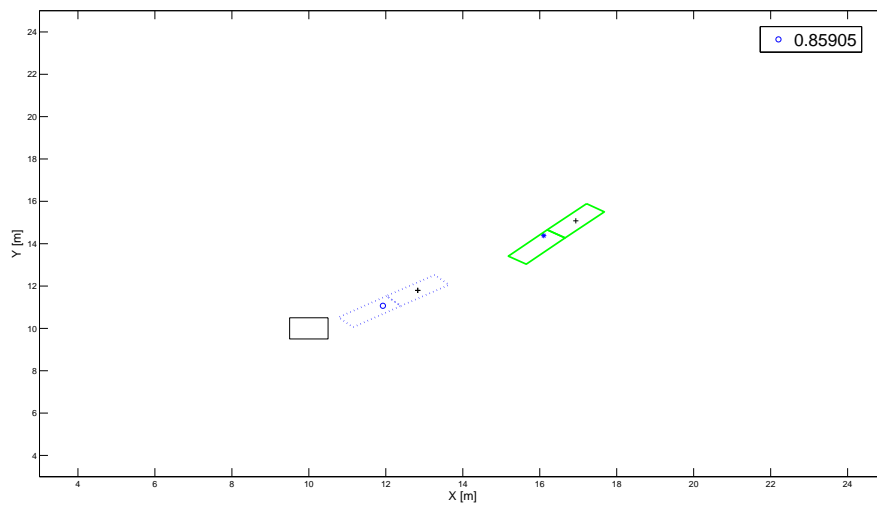


Figure 5-31: The machine here is under normal working condition

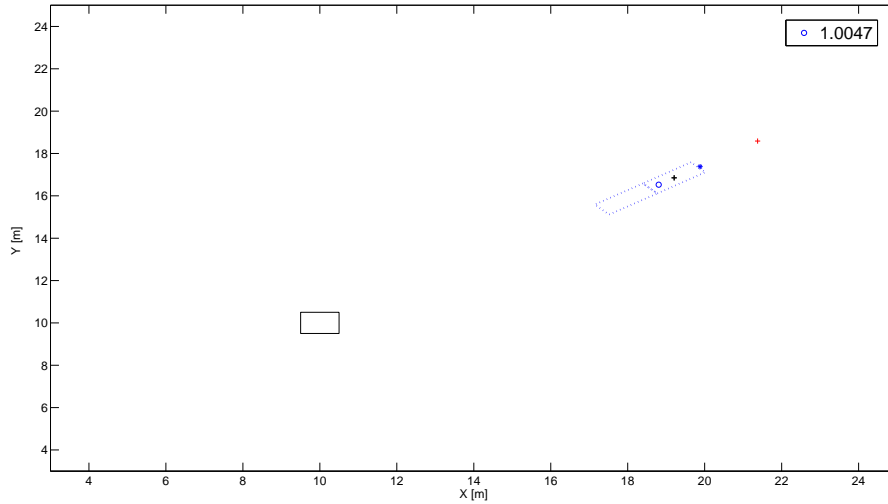


Figure 5-32: The polygon at $t = t_{warn}$ is absent in this figure. This is where the warning is switched off because the position error crosses the threshold value, here the threshold being set at 1 meter.

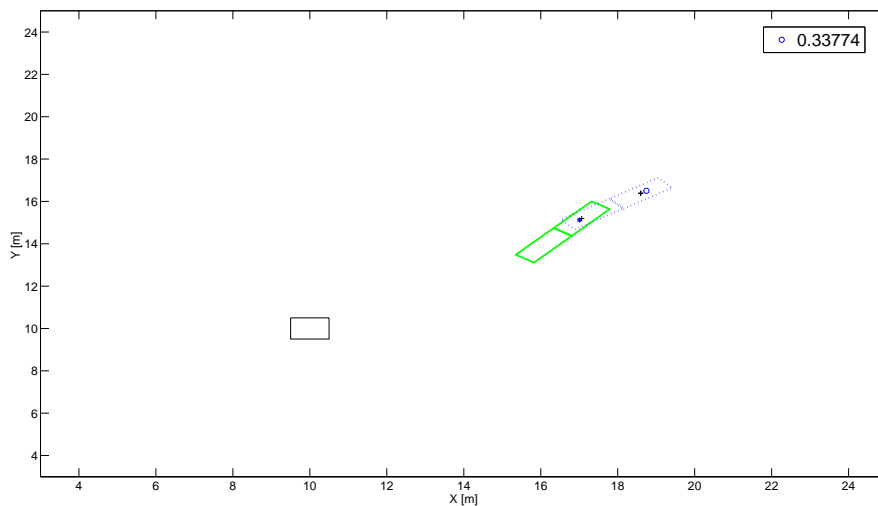


Figure 5-33: Once the position error decreases below the threshold value, the warning is again switched on and the system operates in its normal condition

Conclusions and Future Work

6-1 Results

In this thesis, three important aspects of Collision Avoidance System (CAS) was investigated. First, the problem of model generalization was addressed , second an Extended Kalman Filter (EKF) filter was formulated for estimating the missing states and parameters. Third, a model based deterministic approach was implemented for the threat assessment system.

- A new model was derived which has capability to capture the dynamics of all the three considered models. In order to validate the model, the prediction results of the derived combined machine model were compared with their true machine models. The results show that the model is capable of producing better results than their original models. This is due to the fact that the combined machine model is able to capture more dynamics than the true models.
- An extended kalman filter was formulated for calculating the missing states and parameters of the derived model. The model was validated by comparing the results of the filter with real-time Global Positioning System (GPS) data. Predictions were calculated for two different trajectories (linear and non-linear). A new method was devised which utilized a kalman filter in a iterative way to calculate the predictions. This new method proved to be better performing than the usual prediction method for non-linear trajectories.
- With the help of a predefined warning model, two prediction horizons were formulated taking into consideration the driver's reaction time. A fault detection system was also designed for switching off the warning system when an error is anticipated in the calculated predictions. The result described that the fault is diagnosed but with a delay which depends on the window side (Tuning factor). Finally, a collision detection algorithm was devised which was based on the separating axis theorem which considered the host machine and its future predictions as convex polygons.

6-2 Future Work

1. One of the most important aspect for a efficient CAS is the knowledge about the environment where the machine is operating. This is achieved by equipping the machine with more number of sensors. More sensors (Radar, Lidar, Cameras) other than the GPS units alone can be utilized and with the help of sensor fusion more knowledge about the environment can be obtained. Such systems have proved to be of high capability in todays Trucks and passenger cars. Another way of improvising it is to combine the GPS measurements with the inertial navigation system. According to literature, such systems are very efficient in providing necessary information without the danger of loss of information during GPS outage.

2. Another area which can be investigated more is the threat assessment system where instead of a deterministic approach, probabilistic approach is applied. Probabilistic approach tends to be more computationally heavy but helps in providing better understanding of a risk of a collision [8].

In another approach, the future driver inputs of the surrounding objects can be modeled as random variables. In order to capture realistic driver behavior, a dynamic driver model can be implemented as a probabilistic prior, which computes the likelihood of a potential manoeuver. A distribution of possible future scenarios can be then approximated using Monte Carlo sampling. Based on this distribution, probability of collision or time to collision can be calculated [34].

3. The threat assessment system can be further improved by improvising a gain scheduling controller which could control the deceleration of the vehicle based upon the distance of the machine from the obstacle. This will help in braking the machine with smoother transitions rather than braking the machine instantly causing discomfort to the driver. Furthermore, path planning algorithms can also be integrated with CAS which can help provide more accurate predictions since the machine trajectory will be predefined.

Bibliography

- [1] Insurance Institute for Highway Safety Status Report. Vol. 45, No. 5, May 20, 2010. <http://www.iihs.org/externaldata/srdata/docs/sr4505.pdf>
- [2] Census of Fatal Occupational Injuries *Fatal occupational injuries by selected characteristics, 2003-2012*.. Linköping Studies in Science and Technology. Dissertations, U.S. Bureau of Labor Statistics. http://stats.bls.gov/iif/oshwc/cfoi/all_worker.pdf
- [3] Steven Scheduling, Gamini Dissanayake, Eduardo Mario Nebot, and Hugh Durrant-Whyte, *An Experiment in Autonomous Navigation of an Underground Mining Vehicle*.. IEEE TRANSACTIONS ON ROBOTICS AND AUTOMATION, VOL. 15, NO. 1, FEBRUARY 1999.
- [4] Thaker Nayl, *Modeling, Control and Path Planning for an Articulated Vehicle*.. Department of Computer Science, Electrical and Space Engineering Lulea University of Technology, Lulea, Sweden, June 2013. ISBN 978-91-7439-669-0
- [5] Felipe Nunez, Sergio Navarro, Alberto Aguado, Aldo Cipriano, *State Estimation Based Model Predictive Control for LHD Vehicles*. Proceedings of the 17th World Congress The International Federation of Automatic Control Seoul, Korea, July 6-11, 2008
- [6] Li Pingsheng, Xie Xiaoli, Li Bin, Wang Meng, *The Model of Vehicle Position Estimation and Prediction Based on State-space Approach*. 2009 Second International Conference on Intelligent Computation Technology and Automation, 2009 IEEE DOI 10.1109/ICICTA.2009.664
- [7] Christoffer Noren, *Path Planning for Autonomous Heavy Duty Vehicles using Nonlinear Model Predictive Control*. Department of Electrical Engineering, Linköpings universitet, SE-581 83 Linköping, Sweden. <http://www.control.isy.liu.se>
- [8] Jonas Jansson, *Collision Avoidance Theory with Application to Automotive Collision Mitigation*. Linköping Studies in Science and Technology. Dissertations No. 950. Department of Electrical Engineering, Linköpings universitet, SE-581 83 Linköping, Sweden. ISBN 91-85299-45-6. <http://www.control.isy.liu.se>

- [9] Erik Coelingh, Andreas Eidehall and Mattias Bengtsson. *Collision Warning with Full Auto Brake and Pedestrian Detection - a practical example of Automatic Emergency Braking*. 2010 13th International IEEE Annual Conference on Intelligent Transportation Systems Madeira Island, Portugal, September 19-22, 2010.
- [10] Lee Yang; Ji Hyun Yang; Feron, E.; Kulkarni, V. *Development of a performance-based approach for a rear-end collision warning and avoidance system for automobiles*. Intelligent Vehicles Symposium, 2003. Proceedings. IEEE.
- [11] Yizhen Zhang; Antonsson, E.K.; Grote, K., *A new threat assessment measure for collision avoidance systems*. Intelligent Transportation Systems Conference, 2006. ITSC '06. IEEE
- [12] R. J. Kiefer, D. J. LeBlanc, M. D. Palmer, J. Salinger, R. K. Deering, and M. A. Shulman, *Development and validation of functional definitions and evaluation procedures for collision warning/avoidance system*. CAMP, NHTSA, Final report DOT HS 808 964, August 1999. <http://www-nrd.nhtsa.dot.gov/pdf/nrd-12/acas/HS808964Report-1999-08.pdf>
- [13] O. Khatib., *Real-time obstacle avoidance for manipulators and mobile robots..* The International Journal of Robotic Research, 5, 1986.
- [14] Williams G., Lagace G., and Woodfin A. *A collision avoidance controller for autonomous underwater vehicles..* In Proceedings of the Symposium on Autonomous Underwater Vehicle Technology, pages 206-212, 1990.
- [15] J. Guldner, V. Utkin, H. Hashimoto, and F. Harashima *Obstacle avoidance in rn based on artificial harmonic potential fields..* In IEEE International Conference on Robotics and Automation, volume 3, pages 3051-3056, 1995
- [16] Mohinder S. Grewal, Angus P. Andrews. "*Kalman Filtering: Theory and Practice Using MATLAB., 3rd Edition*". ISBN:978-0-470-17366-4.
- [17] Seller, P., Song, B., Hedrick, J.K., 1998. *Development of a collision avoidance system*. Automotive Engineering International 109, 24-28.
- [18] R.R. Knipling, M. Mironer, D.L. Hendricks, L. Tijeripa, J. Everson, J. C. Allen, and C. Wilson. *Assessment of ivhs countermeasures for collision avoidance: Rear-end crashes..* Technical report, National Highway Traffic Safety Administration, 1993.
- [19] Wilson, T.B., Butler, W., Maghee, V., Dingus, T.A., 1997. *Forward looking collision warning system performance guidelines..* SAE Paper, 970456.
- [20] M. Green. *How long does it take to stop? methodological analysis of driver perception brake times..* Transportation Human Factors, 2(3):195 -216, 2000.
- [21] D. J. LeBlanc, R. J. Kiefer, R. K. Deering, M. A. Schulman, M. D. Palmer, and J. Salinger. *Forward collision warning: Preliminary requirements for crash alert timing..* In Intelligent Vehicle Initiative (Ivi) Technology and Navigation Systems, volume SP-1593, SAE Technical Paper 2001-01-0462, Detroit, MI, USA, March 2001. Society of Automotive Engineers 2001 World Congress..

-
- [22] Christoffer Noren. *Path Planning for Autonomous Heavy Duty Vehicles using Nonlinear Model Predictive Control*. ISRN LiTH-ISY-EX-13/4707-SE <http://www.control.isy.liu.se>
- [23] Eric A. Wan and Rudolph van der Merwe. "The Uncented Kalman Filter". Chapter 7.
- [24] D.V. McGehee, T.L. Brown, J.D. Lee, and T.B. Wilson. *Effect of warning timing on collision avoidance behavior in a stationary lead vehicle scenario..* Journal of the Transportation Research Board, 2007.
- [25] D.V. McGehee, T.L. Brown, and M. Burns T.B. Wilson. *Examination of driver's collision avoidance behavior in a lead vehicle stopped scenario using a front-to-rear-end collision warning system*. Technical report, USDOT/National Highway Traffic Safety Administration, 1993.
- [26] E. Coelingh, M. Distner, M. Bengtsson, and J. Ekmark. *Challenges in low-speed collision avoidance* In 2010 JSAE Annual Congress, 2010.
- [27] Kazuo Tanaka and Takahiro Kosaki. "Design of a Stable Fuzzy Controller for an Articulated Vehicle" IEEE Transactions of Systems, Man, And Cybernetics-Part B: Cybernetics. VOL. 27, NO. 3, June 1997.
- [28] Jochen Teizer, Ben S. Allread, Clare E. Fullerton, Jimmie Hinze. "Autonomous pro-active real-time construction worker and equipment operator proximity safety alert system" Automation in Construction 19 (2010) 630-640.
- [29] Eric MARKS and Jochen TEIZER "Proximity Sensing and Warning Technology for Heavy Construction Equipment Operation" Construction Research Congress 2012, ASCE 2012.
- [30] Melvin L. Myers, *Continuous overturn control of compactors/rollers by rollover protective structures* NIH Public Access. Int J Veh Saf. Author manuscript; available in PMC 2011 July 14.
- [31] Benjamin Scott Allread, "Real Time Pro-Active Safety in Construction" Civil Engineering, Georgia Institute of Technology May 2009..
- [32] Danwei Wang Feng Qi, "Trajectory Planning for a Four-Wheel-Steering Vehicle" Trajectory Planning for a Four-Wheel-Steering Vehicle.
- [33] David Eberly "Intersection of Convex Objects: The Method of Separating Axes" Geometric Tools, LLC <http://www.geometrictools.com/>
- [34] Andreas Eidehall and Lars Petersson. *Statistical threat assessment for general road scenes using Monte Carlo sampling*. In Proceedings of the IEEE Intelligent Transportation Systems 2006, pages 1173- 1178.

Glossary

List of Acronyms

CAS	Collision Avoidance System
GPS	Global Positioning System
MPC	Model Predictive Control
TTC	Time To Collision
EKF	Extended Kalman Filter
SAT	Separating Axis Theorem

